FRK cancer-related mutations: Effect on enzymatic activity and cellular processes

Name: **Josh MacAusland-Berg**

Student ID: 11164060

Program: **MSc. of Biochemistry**

Department: Biochemistry

University of Saskatchewan

Supervisor: **Dr. Kiven Erique Lukong**

PERMISSION TO USE

In presenting this thesis in partial fulfillment of the requirements for a Postgraduate degree from the University of Saskatchewan, I agree that the Libraries of this University may make it freely available for inspection. I further agree that permission for copying of this thesis in any manner, in whole or in part, for scholarly purposes may be granted by the professor or professors who supervised my thesis work or, in their absence, by the Head of the Department or the Dean of the College in which my thesis work was completed. It is understood that any copying or publication or use of this thesis or parts thereof for financial gain shall not be allowed without my written permission. It is also understood that due recognition shall be given to me and to the University of Saskatchewan in any scholarly use which may be made of any material in my thesis.

Requests for permission to copy or to make other use of material in this thesis in whole or part should be addressed to:

Head of the Department of Biochemistry

University of Saskatchewan

Saskatoon, Saskatchewan S7N 5E5

Dean

College of Graduate and Postdoctoral Studies

University of Saskatchewan

116 Thorvaldson Building, 110 Science Place

Saskatoon, Saskatchewan S7N 5C9

Canada

Abstract

Cancer-associated FRK mutations have not been thoroughly studied however, a previous study analyzed six cancer related mutations of BRK L16F, R131L, V253M, N317S, L343F, P450L; and it was found that there are similar residues in FRK. We identified R64P, K87N, S145R, K265R, N359I, del V378-F379 (VF) found in breast cancer, large intestine cancer, ovarian cancer, and liver cancer. This study analyzes the effect of the mutation of these similar residues in the BRK study, as well as uncharacterized cancer related mutations of FRK. Mutating two of the similar residues maintained the same effects in BRK and FRK whereas the remaining mutants in FRK had no effect on activity. The uncharacterized cancer related mutations of FRK produced interesting results where the mutations in kinase domain (K265R, N359I, del VF) reduced, inactivated and increased kinase activity respectively. Proliferation, migration and invasion assays were also performed with the R64P, K265R, N358I and VF mutations. The proliferation data revealed that the cell line expressing wild type FRK reduced cell growth which is consistent with past findings. The other mutations also resulted in reduced cell growth in MDA-MB-231 breast cancer cells but were not significantly different to wild type FRK. The invasion assay results show that the wild type FRK significantly reduced invasion compared to the MDA-MB-231 cells compared to parental controls. Differing from the proliferation assay, the mutations R64P, K265R, N359I, and VF showed no reduction in cell invasiveness compared to the parental. The mutations expressed transiently in HEK293 were found to only impact STAT3 phosphorylation where all FRK constructs induced STAT3 phosphorylation except for N359I. Binding experiments were performed using rotational anisotropy and four peptides derived from FRK C terminus (ETDSS($_p$Y)SDANN), SH2 consensus binding sequence (HF(pY)ENI), PTEN (PNVEEPSNPEASSS), and BRCA1 (DTYLIPQIPHSHY). The wild type SH2 domain was able of binding to both peptides from the FRK C terminus and the SH2 consensus binding sequence with a K_d of 2.5 μM and 0.4 μM respectively. The S145R SH2 domain was also capable of interacting with both peptides with a K_d of 1.4 μM with the FRK C terminus and 0.8 μM with the SH2 consensus binding sequence. Unfortunately, the SH3 domain was unable to bind to the sequences selected.

Acknowledgements

I thank my supervisor Dr. Lukong for his mentorship and guidance in the completion of my MSc degree. I am also grateful to have had a strong support system within the lab including Yetunde Ogunbolude, Aditya Mandapati, Stefany Cornea, and Raghuveera Goel. I also appreciate the assistance and feedback of my committee, Dr. Keith Bonham, Dr. Yu Luo, and Dr. Lukong. I also thank my close friends and family for their faith and support while I spent time in the lab instead of with them.

Table of Contents

List of Figures

List of Tables

List of Abbreviations

APS: Ammonium Persulfate

BRK: Breast tumor kinase

DOK1: Downstream of tyrosine kinases 1

DMEM: Dulbecco's Modified Eagle Medium

DMSO: Dimethylsulfoxide

DTT: Dithiothreitol

EGFR: Epidermal growth factor receptor

GST: Glutathione S-Transferase

GFP: Green Fluorescent protein

HEK293: Human Embryonic Kidney 293

IYK: Intestinal tyrosine Kinase

JNK: c-Jun N-terminal Kinases

MAPK: Mitogen Activated Protein Kinase

PBS: Phosphate Buffered Saline

PBST: Phosphate Buffered Saline with tween

PEI: Polyethyleneimine

PTEN: Phosphatase and Tensin Homolog deleted on chromosome 10

PMSF: Phenylmethanesulfonyl fluoride

SH2: Src-homology 2

SH3: Src-Homology 3

SRMS: Src Related tyrosine kinase lacking C terminal Regulatory tyrosine and N terminal myristoylation sites

STAT3: Signal transducer and activator of transcription 3

Overview

The main objectives of this project were to investigate the effect caused by FRK cancer-related mutations. I will address these objectives by analyzing cell proliferation, migration, invasion and signaling. In addition, I will determine how these mutations affect substrate binding.

1.0 Introduction

1.1 Cancer and Tyrosine Kinases

Cancer arises from a series of mutations that dysregulate the cells response to extracellular signals and allow the cell to grow without outside signaling (Hanahan and Weinberg, 2011). Tyrosine kinases mediate the response to growth signaling factors (Hanahan and Weinberg, 2011). Their activity is strictly regulated in normal cells but can acquire transforming roles due to mutations which result in increased cell proliferation, migration and invasion. Transforming activity can be caused from mutations, fusions, or amplifications. Mutations in EGFR which lack amino acids 6-273, give the receptor constitutive activation (Zalutsky, 1997). The BCR-Abl fusion has been studied in CML where the first exon if Abl is replaced with BCR sequences which results in constitutive activity (An et al., 2010). Lastly, amplification is a mechanism which heightens activity due to increased protein level. Proteins such as HER2 which is overexpressed in certain breast cancers due to gene amplification and EGFR which is over expressed in a series of cancers (Menard et al., 2000). Tyrosine kinases have been seen to play critical roles in cancers and have become major therapeutic targets which shows the importance of this protein family in both normal and cancer cells.

1.2 Tyrosine Kinases:

Tyrosine kinases are a diverse group of proteins which play a role in a number of cellular processes through the mediation of signaling cascades such as growth, differentiation, migration, invasion, apoptosis and metabolism (Paul and Mukhopadhyay, 2004). This family is made up of 90 total proteins and is divided into two major groups; receptor tyrosine kinases (RTK) and non-receptor tyrosine kinases. Of these 90 tyrosine kinases, 58 are receptor tyrosine kinases which form 20 subfamilies and 32 are non-receptor (NRTK) which are organized into 10 different subfamilies (Robinson et al., 2000). The RTKs are membrane spanning proteins which possesses a ligand binding site on the extracellular side and a kinase domain on the intracellular side than participates in auto and transphosphorylation following ligand binding and dimerization. Non-receptor tyrosine kinases are cytosolic kinases whose structure and localization can vary. The kinase domain of the NRTKs spans approximately 300 amino acid residues and form 2 distinct lobes, the N and C lobes. The binding site for ATP is located in a cleft in between the two lobes (Paul and

Mukhopadhyay, 2004). The RTKs are the starting point of signaling events in response to extracellular signals where the NRTKs participate in signaling events downstream of the RTKs.

1.2.1 SRC Family Kinases:

The Src family of tyrosine kinases (SFKs) is perhaps the best studied group of tyrosine kinases. This family of kinases plays critical roles in cell signaling, cell division, motility, adhesion, angiogenesis and survival (Summy and Gallick, 2003). The Rous Sarcoma Virus, which is capable of generating tumors within chickens, was first discovered in 1911 by Peyton Rous (Rous, 1911). The transforming characteristics of this virus were found to be induced by a protein called Src. There were also two variants of this gene, v-Src the oncogene, and c-Src the proto oncogene (Smart et al., 1981). V-Src is an unregulated form of Src which lacks a C-terminal tail and regulatory tyrosine. The SFK is made up of 9 NRTKs those being, c-Src, c-Yes, Fyn, Lyn, Lck, Hck, Blk, Fgr, and Yrk. This family of proteins is distinguished by the presence of three conserved domains, the SH3, SH2, and Kinase domains as well as eleven exons (Cetkovic et al., 2004).

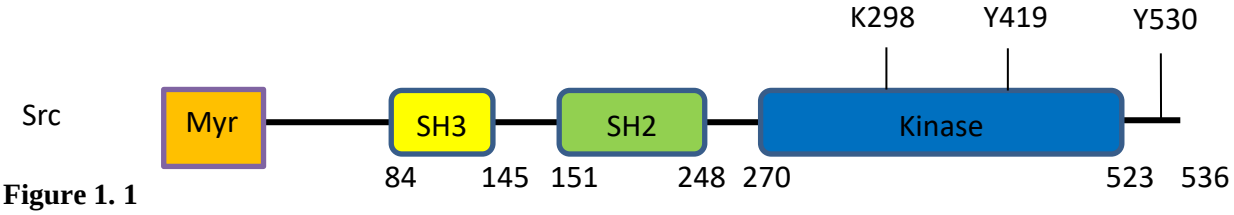

Figure 1. 1

Src structure schematic showing SH3, SH2, and kinase domains and N terminal myristoylation site. Numbers on the bottom indicate the starting and ending amino acid residue for each respective domain and numbers on top indicate important residues. Lysine 298 (K298) is the ATP contacting residue, Tyrosine 419 (Y342) is the autophosphorylation site and Tyrosine 530 is the C terminal regulatory tyrosine.

1.2.2 Src Regulation:

C-Src is regulated through phosphorylation of a specific tyrosine residue Y530 in the C-terminal tail which is conserved in other family members (Cooper et al., 1986).When Y530 becomes phosphorylated, the C-terminal tail can interact with the SH2 domain of c-Src. This interaction between the C-terminus and the SH2 domain lock c-Src in an inactive conformation. The SH3 domain also interacts with the poly-proline rich region between the SH2 and kinase domain in order to aid repression of enzymatic activity (Cooper et al., 1986; Cooper and Howell, 1993). An additional critical tyrosine was also identified, which when phosphorylated causes c-Src to become active. This tyrosine is Y419 located within the kinase domain (Jove and Hanafusa, 1987).

Additional conserved amino acids are also found in the kinase domain of Src. The lysine 298 is responsible for the interaction with ATP where the kinase domain can then facilitate the breakdown of ATP to ADP and phosphorylate its target tyrosine (Luttrell et al., 1996). Src possesses an N-terminal myristoylation site but all of the Src family kinases possess either myristoylation or palmitoylation signals which localizes the NRTK to the membrane where it can interact with its targets (Buss et al., 1986).

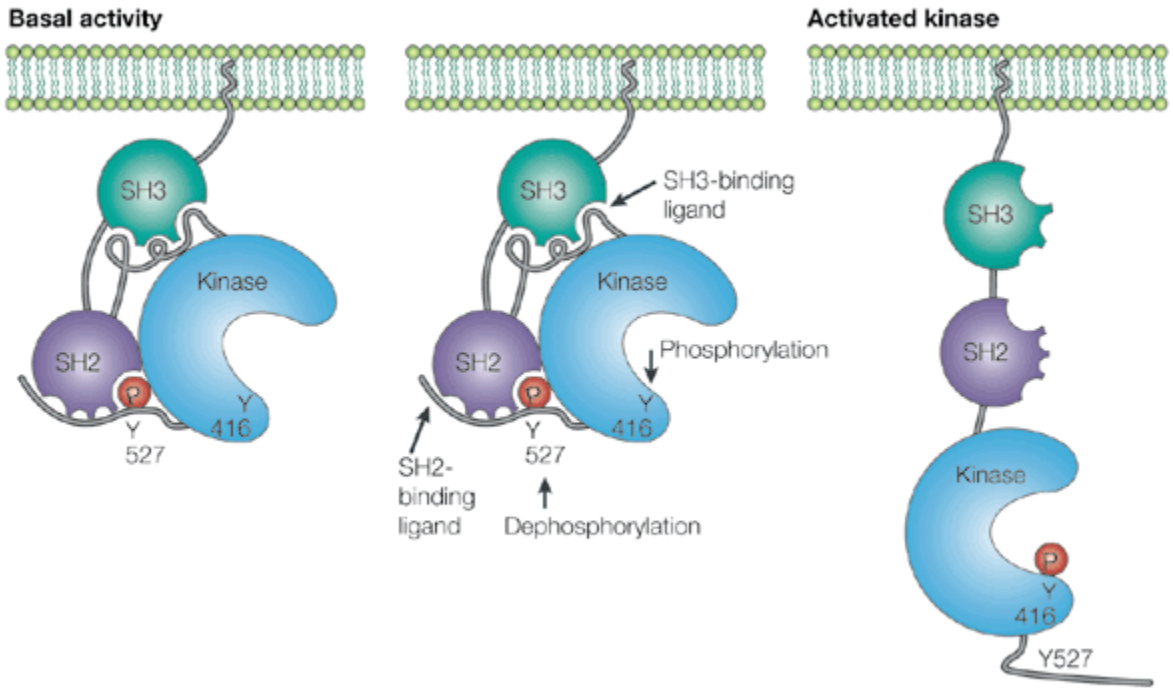

Figure 1. 2

Regulation of the Src kinase through phosphorylation. As presented when tyrosine 527 (530 in Humans) becomes phosphorylated and interacts with the SH2 domain. The SH3 domain then interacts with a region between the SH2 and kinase domain. Intramolecular interactions between the SH3 and SH2 domain lock the enzyme in an inactive conformation. This inactivation can be reversed through the dephosphorylation of tyrosine 527 and the enzyme can become active through the autophosphorylation of tyrosine 416 (Y419 in Humans) (Martin, 2001).

1.2.3 SH3 Domain:

The Src homology 3 (SH3) domain is conserved among all Src family and related kinases. This domain is roughly 60 amino acids in length and was first identified towards the N terminus separate from the catalytic domains in Src tyrosine kinases (Mayer et al., 1988). This domain facilitates interactions of SFKs with signaling receptors and participate in inter/intramolecular interactions. SH3 domains are composed of a five stranded β-sandwich and a short helix (Saksela and Permi, 2012). The original consensus sequences was identified to be PXXP (P being proline and "X" being any of the 20 amino acids) (Ren et al., 1993). It was also found that the PXXP motif could bind in two different conformations depending on the placement of a positive amino acid such as lysine or arginine (Feng et al., 1994; Yu et al., 1994). The two orientations are K/RxxPxxP or xPxxPxK/R which are referred to as type I and type II respectively (Lim et al., 1994). Both of these peptide types possess the PxxP base motif and binds to SH3 domains which is mainly hydrophobic due to the surface aromatic amino acids (Lim et al., 1994). There also exists an additional binding pocket referred to as the specificity pocket which will bind to the N terminus of the type I peptide and the C terminus of the type II peptides. This pocket interacts with the positively charged amino acids of either type I or type II peptides and is therefore negatively charged (Feng et al., 1994).

The PI3K SH3 domain has been bound to a type II peptide and structure based mutations were generated (Yu et al., 1994). Since both PI3K and Src bind peptides with N terminal arginines mutations of conserved residues between PI3K and Src were generated to observe changes in peptide binding. The peptide RKLPPRPSK was referred to as RP1 by Yu *et al*. (1994) and the acidic residues of the domain which interact with the first and sixth arginine were mutated. These mutations were E19Q D21N, E51Q in PI3K with those residues also being conserved in Src. It was found that the aspartate mutations D21N had the most drastic effect on peptide affinity where the K_D was far increased indicating a less tight interaction (Yu et al., 1994).

1.2.4 SH2 Domain:

The Src homology 2 (SH2) domain, much like the SH3 domain is a non-catalytic domain of approximately 100 amino acids in length that is associated with the interaction of SFKs with signaling receptors and molecules as well as intramolecular interactions (Russell et al., 1992; Sadowski et al., 1986). These domains have been found in all SFKs, but also a number of signaling

molecules near the plasma membrane which facilitate the intracellular transduction of extracellular signals. The structure of this domain is relatively conserved with a five stranded anti-parallel β-sheet core sandwiched between two alpha helices extended by a β-strand and small triple stranded β-sheet (Waksman et al., 1992). Sequence alignment studies have also been performed and show a short sequence of six amino acids was found to be highly conserved. That sequence in Src is FLVRES and FLIRES in FRK (Campbell and Jackson, 2003). Of the conserved motifs, this sequence has been implicated in the facilitation of phosphotyrosine binding. Certain amino acids in this conserved sequence may play a larger role in phosphotyrosine binding. The arginine of this motif was mutated in Src and resulted in the inhibition of phosphotyrosine binding (Bibbins et al., 1993). The serine had also been mutated in Abl kinase where it then lost its ability to transform fibroblasts where the wild type Able kinase was capable of initiating transformation. It was reasoned that the inability to transfom fibroblasts was reduced binding to phosphotyrosines (Mayer et al., 1992). Several of the amino acids in the sequence FLVRESES in Src were mutated and seen to have decreased phosphotyrosine binding those mutations with proposed reduced binding were R171K, S173C, and S175C. the arginine was seen to have the greatest inhibition of phosphotyrosine binding (Mayer et al., 1992).

Peptide specificity is quite variable across the different tyrosine kinase families and signaling molecules. A study in 2013 analyzed the differing sequence specificities of a number of Src related kinases including FRK, BRK and SRMS (Zhao et al., 2013). This study used randomized peptides in the order xxpYxxx, with the x indicating any of the 20 amino acids from the -2 position to the +3 position with the phosphotyrosine at position 0. Src was found to preferentially bind to HYpYTMI, FRK to HFpYENI, BRK to HMpYDIC, and SRMS to HHpYHIC.

1.3 BRK Family Kinase:

The BRK family kinases (BFK) include three non-receptor tyrosine kinases which include FRK, BRK and SRMS. These three tyrosine kinases do not share a great deal of sequence similarity but are grouped together because of similar gene-splicing patterns. Src family kinases possess 11 exons where FRK, BRK, and SRMS are comprised of 8 exons (Goel and Lukong, 2015; Serfas and Tyner, 2003). Much like the SFK family, the three BFK members possess SH3, SH2, and kinase domains (Goel and Lukong, 2015; Serfas and Tyner, 2003). The SH3 and SH2 domains are both non-catalytic and interact with protein targets, where the kinase domain functions to

phosphorylate the enzymes target tyrosine through the conversion of ATP to ADP. All three proteins in this family lack a myristoylation site which are found at the N-terminus of SFKs and are critical for their membrane association (Goel and Lukong, 2015; Serfas and Tyner, 2003).

1.3.1 Breast Tumor Kinase (BRK):

Breast tumor kinase (BRK) also known as PTK6 is a non-receptor kinase 451 amino acids in length and maps to chromosome 20. This enzyme is composed of 3 functional domains where the two N terminal domains, the SH3 and SH2 domains facilitate protein-protein interactions and the kinase domain phosphorylated its target substrate through the breakdown of ATP. Several amino acids are conserved through this family such as the ATP binding lysine and the autophosphorylation tyrosine. K219 is responsible for ATP binding and Y342 is the autophosphorylation site. BRK has oncogenic effects when over expressed in breast cancer and it has also been found that BRK is over expressed in over 80% of breast cancers, while it is not expressed in normal mammary glands (Barker et al., 1997). Regulation also occurs in a similar manner to the regulation of Src, where in BRK's case tyrosine 342 is the autophosphorylation site and must be phosphorylated to become active. Tyrosine 447, located in the C terminus is the regulatory tyrosine and when phosphorylated interacts with the SH2 domain of BRK and locks the enzyme in an inactive conformation (Qiu and Miller, 2002).

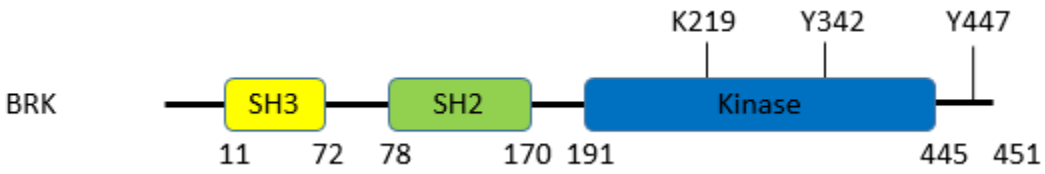

Figure 1. 3

Breast tumor kinase (BRK) showing SH3, SH2, and kinase domains. Numbers on the bottom indicate the starting and ending amino acid residue for each respective domain and numbers on top indicate important residues. Lysine 219 (K219) is the ATP contacting residue, Tyrosine 342 (Y342) is the autophosphorylation site and Tyrosine 447 is the C terminal regulatory tyrosine.

This tyrosine is also conserved with FRK and SFKs. BRK null mice have also been generated in the past by the Tyner group (Haegebarth et al., 2006). BRK is expressed in healthy gut intestinal tissue, which is where the effects were noticed. There were increased rates of growth as the intestinal villi appeared longer than wild type. Also noted was a slower differentiation where

samples from the intestines of these mice showed decreased levels of intestinal fatty acid binding protein (Haegebarth et al., 2006). In 2012 a xenograft study was performed by the Lukong lab where wild type BRK and BRK Y447F, the constitutively active mutation, were stably expressed in MDA-MB-231 breast cancer cells and injected into mouse mammary fat pads (Miah et al., 2012). Wild type BRK was capable of produce a slightly larger tumor than the control MDA-MB-231 cell line, and the BRK Y447F mutation produced tumors three-fold larger than in the control mice. This indicates the BRK must be fully activated for these effects to be seen (Miah et al., 2012).

1.3.2 Src Related Kinase Lacking C Terminal Tyrosine and N Terminal Myristoylation Sites (SRMS):

SRMS is a non-receptor tyrosine kinase 488 amino acids long and maps to chromosome 20 adjacent to BRK (Kohmura et al., 1994). This kinase also possesses Src homology domains, SH3, SH2 and the kinase domain but lacks a C terminal tail. The lack of a C terminus indicates an alternative mechanism for enzymatic regulation. The SH3 and SH2 domains participate in protein-protein interactions and the kinase domain phosphorylates SRMS' target substrates. The amino acids responsible for ATP binding and autophosphorylation have been identified. K258 has been shown to interact with ATP and Y380 as the main autophosphorylation site required for activity. Mutation of K258 resulted in reduced autophsphorylation and mutation of Y380 resulted in reduced activity. SRMS is the most understudied protein of the BFKs and as a result its main function remains unknown. BRK and FRK have been studied closer than SRMS and their functions are somewhat understood. BRK has been seen to function as an oncogene and FRK is a candidate tumor suppressor in breast tissue. The Lukong lab has recently conducted a study on SRMS concerning its expression in breast cancer and its association with Dok1 (Goel et al., 2013). The study concluded that SRMS is overexpressed in breast cancer compared to the normal tissue. Also, that SRMS is an active kinase whose activity is regulated through interactions that requires its N terminus. Lastly Goel et al. determined that Dok1 is in fact a substrate of SRMS (Goel et al., 2013).

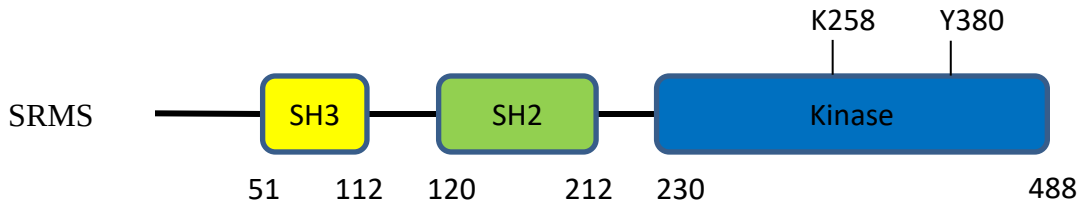

Figure 1. 4

Src Related Kinase Lacking C Terminal Tyrosine and N Terminal Myristoylation Sites (SRMS) exhibiting its SH3, SH2 and kinase domains, extended N terminus and lack of a C terminus. Numbers on the bottom indicate the starting and ending amino acid residue for each respective domain and numbers on top indicate important residues. Lysine 258 (K258) is the ATP contacting residue, and Tyrosine 380 (Y380) is the autophosphorylation site. There is no regulatory tyrosine present as there is no C terminus however, SRMS' N terminus is required for activity.

1.4 Fyn Related Kinase (FRK):

1.4.1 Gene Discovery

FRK, also known as Rak, the Russian word for cancer, is a 54 kDa non-receptor tyrosine kinase which maps to the chromosomal locus 6p21-23 which is frequently deleted in cancer (Goel and Lukong, 2016). FRK was discovered in breast cancer through a search for novel kinases where conserved sequences of known kinase catalytic domains were used to amplify similar sequences of unknown kinase domains in order to identify them first named TKI along with additional kinase discovered. FRK was then cloned in a later study through polymerase chain reaction (PCR) from the liver cancer cell line HEP3B (Lee et al., 1994). This was done using primers which were based off tyrosine kinase (TYK) motifs. The product of these PCR reactions resulted in a 180 bp fragment which was then used to amplify full length cDNA. These resulting clones were a length of 2.9 kb and coded for a protein 505 amino acids in length. Several features were noticed which suggested that FRK functions as a kinase. Those being an ATP binding domain and a conserved motif (DLAARN) which suggested that FRK was a TYK and not a serine/ threonine kinase. The Src kinase family all possess SH3, SH2 and kinase domains, and both SH3 and SH2 domains were identified in FRK. The gene was also lacking a hydrophobic stretch of residues which place this kinase into the non-receptor group of TYKs. It was found that FRK possessed a 49% amino acid

sequence similarity to Fyn kinase and a 47% identity to c-Src, and for that reason it was named Fyn-Related-Kinase (FRK) (Lee et al., 1994).

1.4.2 Structure

FRK is a 505 amino acid protein which is related to Src through its SH3, SH2 and kinase domains and is part of the BRK family of kinases which also includes BRK and SRMS. The SH3 and SH2 domains are involved in protein-protein interactions. The SH3 domain will interact with the motif PXXP, while the SH2 domain will bind to phosphorylated tyrosines. There is a nuclear localization signal within the SH2 domain of FRK (KRLDEGGFFLTRRR) although it is expressed in the cytosol of epithelial cells (Cance et al., 1994). Several amino acids which are critical for function were also characterized. The study which initially identified FRK where they first analyzed its activity it was found that FRK was an active kinase with an auto phosphorylation site on tyrosine 387 (Cance et al., 1994).

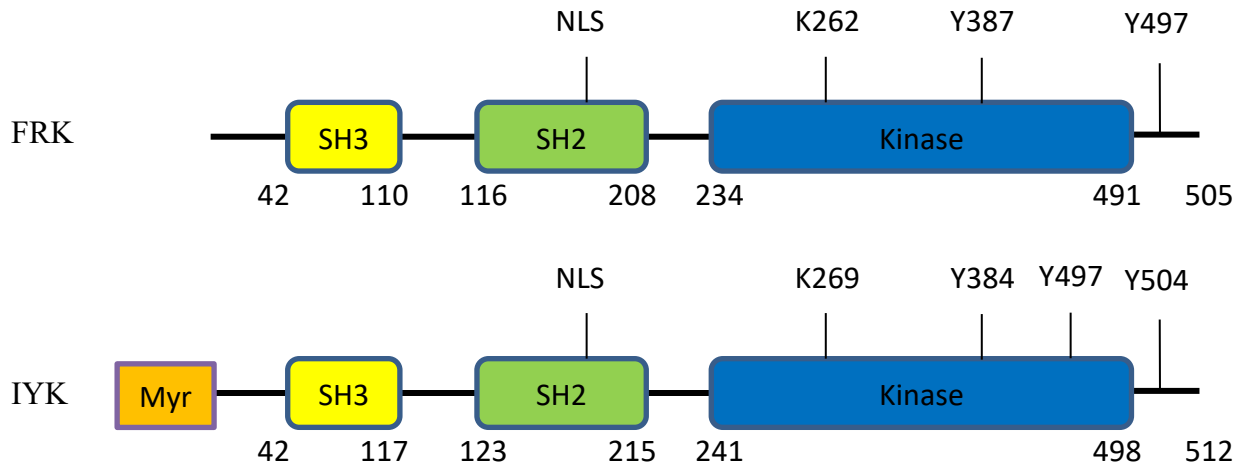

Figure 1. 5

Structure schematics of FRK and mouse ortholog IYK exhibiting SH3, SH2 and kinase domains. Also labelled is a nucleus localization site within the SH2 domain (NLS). Numbers on the bottom indicate the starting and ending amino acid residue for each respective domain and numbers on top indicate important residues. Lysine 262 (K262) is the ATP contacting residue, Tyrosine 387 (Y387) is the autophosphorylation site and Tyrosine 497 is the C terminal regulatory tyrosine. IYK possesses an N terminal myristoylation site as well as critical amino acids labelled Lysine 269 (K269) is the ATP contacting residue, Tyrosine 384 is the autophosphorylation site and Tyrosines 497 and 504 (Y4987, Y504) are regulatory tyrosines.

FRK may be regulated in a similar manner to Src and BRK, where the C-terminal tyrosine 497 binds to the SH2 domain once phosphorylated and the SH3 domain interacts with the SH2-Kinase linker region. This locks the enzyme in an inactive conformation preventing FRK from phosphorylating its target proteins. Studies have been performed on IYK, the mouse ortholog of FRK in which mutation of the C terminal tyrosine resulted in decreased activation (Oberg-Welsh et al., 1998). Although there are similarities between FRK and IYK, one noticeable difference is that IYK possesses an N terminal myristoylation site where FRK does not. This could indicate that the mouse FRK ortholog may have differing functions to FRK (Serfas and Tyner, 2003). Additional amino acid residues are conserved between these family members, those being the ATP binding lysine and autophosphorylation site located in the kinase domain (Figure 1). The autophosphorylation site (Y387 in FRK) must be phosphorylated for FRK to be fully activated. Lysine 262 is the residue responsible for ATP bind and mutation of K262 in FRK results in an inactive enzyme due to the loss of ATP binding (Cance et al., 1994; Meyer et al., 2003). There is also a highly conserved tryptophan (W227 in FRK) residue in the BFK family. Mutating this conserved tryptophan residue in BRK and SRMS results in an inactive enzyme. It is speculated that this residue interacts with the N lobe of the kinase and promotes its stability (Goel et al., 2013). The proteins in the BRK family may have differing functions as BRK has been described as an oncogene where it is overexpressed in 60% of breast cancers (Brauer and Tyner, 2010)where FRK behaves as a tumor suppressor in breast cancer and glioma cell lines due to its growth inhibitory effects (Goel and Lukong, 2016). SRMS is the last member of this family however its main roles have not yet been elucidated.

1.4.3 FRK Tumor Suppressor Role:

The expression of FRK is decreased or lost in some breast cancers and gliomas, which may indicate its role as a potential tumor suppressor (Bagu et al., 2017; Zhou et al., 2012). The mechanism of the loss of FRK expression was investigated by our lab and it was found that promoter hyper-methylation was responsible for the lost expression (Bagu et al., 2017). Localization also plays a large role in the functionality of this kinase in terms of modulating signaling in these cell lines. FRK has a nuclear localization signal in its SH2 domain however; it is detected primarily in the cytosol of breast cancers. Nuclear FRK may be responsible for its growth inhibitory function as it

is localized to the cytosol in the proliferative follicular phase of the menstrual cycle and localized to the nucleus post ovulation during the luteal phase (Berclaz et al., 2000). FRK has also been seen to interact with Phosphatase and tensin homolog (PTEN) in breast cancer which is a negative regulator of AKT signaling (Brauer and Tyner, 2009). PTEN functions by dephosphorylating phosphatidylinositol 3, 4, 5 tri phosphate (PIP3) which prevents AKT activation. FRK phosphorylates PTEN on Y336 and this phosphorylation prevents PTEN from being degraded by NEDD4 and results in reduced activation of AKT signaling and reduced cell proliferation (Brauer and Tyner, 2009). Much like the interaction with PTEN, FRK phosphorylated BRCA1 on Y1552 which prevents proteasome mediated degradation of BRCA1 (Kim et al., 2015). This phosphorylation of BRCA1 by FRK prevents the accumulation of DNA damage (Kim et al., 2015). An interaction has also been seen between FRK and EGFR. EGFR function can be modulated through phosphorylation of tyrosine 1173 by FRK. This phosphorylation event may reduce EGFR activity through the reuptake of EGFR into vesicles and degradation. When analyzing how FRK binds to EGFR it was found that deletion of either the SH3 or SH2 domain resulted in a stronger interaction between FRK and EGFR. The significance of this remains unknown (Jin and Craven, 2014). FRK may function as a tumor suppressor in glioma as it has been seen to decrease the levels of phospho JNK and c-Jun (Zhou et al., 2012). Growth inhibitory effects have also been seen in glioma where FRK prevents nuclear cyclin D accumulation which promotes G1 cell cycle arrest (Hua et al., 2014). The expression of FRK also increased the levels of N-cadherin in glioma thus promoting the N-cadherin/ b-Catenin complex. This interaction results in decreased cell proliferation, and migration (Shi et al., 2015).

1.4.4 FRK Oncogenic Role:

Although the majority of studies exhibit FRK's tumor suppressor role in breast cancer and glioma, a study was performed investigating FRK's role in liver cancer. This study analyzed a number of FRK activating mutations located in the kinase domain which suggest that FRK may function as an oncogene in hepatocellular carcinoma. The activating FRK mutations del V378-F379 and del V378-K380 produced high levels of phosphorylated STAT3 and were capable of forming tumors in xenograft mouse models (Pilati et al., 2014).

Several FRK fusion proteins have been identified which possess oncogenic properties. A fusion protein between ETV6 and the kinase domain of FRK was identified in a patient with acute

myelogenous leukemia (AML). In this fusion protein, exon 4 of ETV6 is fused to exon 3 of FRK which comprises the oligomerization domain of ETV6 and the kinase domain of FRK. It was found that ETV6/FRK could transform Ba/F3 and NIH3T3 cells in a kinase dependent manner indicating that this fusion protein can contribute to leukemogenesis (Hosoya et al., 2005).

A second FRK fusion protein has been identified with Caprin1 in ALK-negative anaplastic large cell lymphoma (ALCL). Caprin1 is a cell cycle associated protein that is expressed in lymphocytes and found expressed in ALCLs. In this case Caprin1 has become fused to exon 3-8 of FRK, with a break point at residue 156 in the SH2 domain. The fusion between Caprin1 and FRK was capable of inducing STAT3 phosphorylation in Ba/F3 and HEK 293T. It was also noted that the function of this fusion protein was inhibited by the kinase inhibitor dasatinib, which may indicate that these FRK rearrangements could be possible candidates for novel therapeutic treatments (Hu et al., 2018).

1.4.5 FRK Interaction Partners:

FRK has been confirmed to interact with proteins such as PTEN, EGFR, and BRCA1. The SH2 domain of FRK has also been characterized for its binding specificity through binding a phosphotyrosine peptide with random amino acids in positions -2 to +3 with the phosphotyrosine at position 0. The preferred peptide of the FRK SH2 domain is HFpYENI. There is also some overlap in the amino acid sequence of the preferred peptide between the three BFK members, but certain residues will dictate how the FRK SH2 domain forms interactions with its specific binding partners (Zhao et al., 2013).

The retinoblastoma protein (pRB) was the interaction of FRK that was first characterized that yielded the first possibility that FRK was a tumor suppressor since the transfection of FRK into NIH 3T3 cells resulted in a reduced number of colonies being formed (Craven et al., 1995). pRB is a protein which functions to regulate the cell cycle, through the binding of E2F thus inhibiting their function. This keeps the cell in the G1 phase (Weinberg, 1995). This regulation of cell cycle and repression of E2F occurs when pRB is hypophosphorylated, however, CDK4/Cyclin D form a complex where it phosphorylates pRB. When pRB is hyperphosphorylated it can no longer bind E2F and the cell cycle is allowed to proceed (Weinberg, 1995). FRK was seen to associate with pRB within the A/B pocket. The significance of this interaction has not yet been elucidated

however speculation may suggest that this interaction brings FRK into proximity of other targets (Craven et al., 1995).

The interaction between FRK and phosphatase and tensin homolog deleted from chromosome 10 (PTEN) has been previously characterized. PTEN is a tumor suppressor gene located on chromosome 10 that is frequently deleted in a number of cancers including breast cancer (Li et al., 1997). PTEN functions to inhibit the AKT signaling pathway, where PTEN's phosphatase activity dephosphorylates phosphatidylinositol 3, 4,5-triphosphate which regulates the activity of AKT and represses the cell survival and growth initiation responses (Cantley and Neel, 1999). It was discovered that FRK interacted directly with PTEN through the SH3 domain of FRK and the C2 domain or phosphatase domain of PTEN (Yim et al., 2009). Yim *et al*. also characterized the phosphorylation of PTEN by FRK on tyrosine residue 336 which resulted in the increased stability and decreased association with NEDD4 which reduces degradation of PTEN (Yim et al., 2009).

EGFR EGFR (epidermal growth factor receptor) has also been studied as an interaction partner of FRK. is a membrane spanning ligand receptor tyrosine kinase that upon stimulation with its ligand (EGF) EGFR receptors dimerize and participate in auto and transphosphorylation. This receptor tyrosine kinase then functions as a docking site for proteins such as Grb2 which further transduces extracellular signals (Giubellino et al., 2008). Jin and Craven revealed that there was a direct interaction between FRK and EGFR (Jin and Craven, 2014). Experiments similar to the PTEN interaction study were then conducted where domain deletions of FRK were constructed in order to identify which domain participated in the interaction. When either the SH3 or SH2 domains were deleted it did not alter the interaction between FRK and EGFR although only the simultaneous deletion of both binding domains resulted in a decreased interaction. This result suggests that the domains must bind to EGFR cooperatively in order to interact with EGFR. Phosphorylation of tyrosine 1173 on EGFR contributes to the internalization of the membrane receptor (Keilhack et al., 1998; Sorkin and Goh, 2009). FRK was shown to phosphorylate this tyrosine residue and reduce the concentration of EGFR at the plasma membrane (Jin and Craven, 2014)

Recently FRK was noted to interact with tumor suppressor BRCA1 in a similar manner to PTEN. BRCA1 is a tumor suppressor that plays critical roles in the cell cycle, DNA repair and apoptosis (Snouwaert et al., 1999; Thangaraju et al., 2000; Xu et al., 2001). Kim et al. have shown that the

loss of FRK results in an increase of detectable DNA damage and impaired double stranded break (DSB) repair in MCF10a (Kim et al., 2015). They also noted that increased FRK expression correlated with increased BRCA1. Again, similar deletion constructs of FRK SH3 and SH2 domains were generated to identify the important domain for interaction with BRCA1. The interaction was no capable of forming when lacking the SH3 domain which means that domain is key for this interaction. And much like PTEN FRK was observed phosphorylating tyrosine 1152 of BRCA1 which enhances its stability through reduced interaction with UBE2T, which is a ubiquitin ligase (Kim et al., 2015).

1.4.6 Mouse Models:

A number of studies have been conducted where FRK has been knocked out using mouse models. FRK may function as a tumor suppressor however; its functions may overlap with another tyrosine kinase as frk-null mice are viable and display no histological abnormalities in epithelial tissues. Decreased levels of T3 hormone were seen but the significance of this is not understood. The frk-null mice were monitored for two years and did not form spontaneous tumors or altered response to ionizing radiation (Chandrasekharan et al., 2002).

A model addressing FRKs tumor suppressing function was generated using the MCF-10a cell line which is a normal breast epithelial cell line (Yim et al., 2009). MCF10a cells express FRK so the experiment was designed with the parental cell line as the control and an FRK knock down cell line. The parental cell line was unable to form tumors but, when FRK had been knocked down using a shRNA, tumors were able to form (Yim et al., 2009).

1.5 Cancer-associated mutations in BFK family members, BRK and FRK:

The BFK family member BRK has been studied extensively, and in 2015 a series of cancer associated mutants were analyzed for their effect on activity, signaling, cell proliferation and migration and substrate recognition (Tsui and Miller, 2015). Of the six mutants analyzed one was located in the SH3 domain (L16F), one was located in the SH2 domain (R131L), three were located in the kinase domain (V253M, N317S, L343F), and one was located in the C terminal tail (P450L). Of these BRK mutants, L16F, R131L, L343F and P450L all displayed increased enzymatic activity compared to wildtype BRK activity. This study revealed that a number of cancer associated mutants varyingly effect the kinase activity of BRK. This altered activity also affects BRK

regulated processes, which result in atypical substrate recognition, cell proliferation, migration, and invasion (Tsui and Miller, 2015). Like BRK, cancer associated mutations have also been identified in FRK with implications not only on FRK enzymatic activity but also its cellular functions. Pilati *et al*. identified FRK gain-of-function mutations, all of which were found in the FRK kinase domain (**Table 1**). Similarly, we found that certain residues in FRK were conserved with those found to be mutated in BRK in patient cancer tissues. It is therefore likely that these residues are also functionally conserved and important to study in the context of FRK enzymatic activity and FRK cellular functions. Unique cancer associated mutations of FRK will also be analyzed, those being R64P, K87N, S145R, K265R, N359I, and VF.

A SRMS null mouse model has also been generated to uncover the physiological importance of SRMS (Kohmura et al., 1994). Kohmura *et al*. determined that the SRMS knockout mice were viable and fertile. No obvious abnormalities were found (Kohmura et al., 1994).

1.6 Cell Signaling

1.6.1Mitogen Activated Protein Kinases (MAP Kinases)

MAP kinases are a family of serine/threonine kinases which control signaling pathways that transduce extracellular signals including response to hormones, or activation of signaling receptor kinases (Pearson et al., 2001). MAP kinases are divided into three levels (MAP3K, MAPKK, and, MAPK) which is held together to important cellular organelles through the use of scaffold proteins (Pimienta and Pascual, 2007). The MAP3K are activated at the cell membrane then function to phosphorylate MAPKK which phosphorylate MAPKs which then are capable of entering the nucleus to alter gene transcription depending on the initial signal (Pimienta and Pascual, 2007).

The first well studied MAP kinase pathway was the Ras-Raf pathway which is important for cellular functions such as differentiation and cell proliferation, however, if left unregulated this pathway can provide growth signals to cancer cells (Avruch et al., 2001). The Ras protein is a guanosine triphosphatase (GTPase) which binds both GDP and GTP and has low intrinsic GTP hydrolysis (Wennerberg et al., 2005). Guanine nucleotide exchange factors (GEF) replace the GDP within RAS to GTP for RAS to become fully active. This GTPase is localized to the membrane where it can respond and transduce a variety of extracellular signals to downstream effectors (Wennerberg et al., 2005). Ras is activated after receptor tyrosine kinases have interacted with a

ligand which results in dimerization and auto and transphosphorylation. These phosphorylation events allow GEFs to bind through their SH2 domains and activate RAS. Ras then recruits PI3K which in turn activates AKT leading to a series of cell signaling events that lead to cell survival through MAP kinases (Mor and Philips, 2006).

1.6.2 Signal Transducer and Activator of Transcription 3 (STAT3) Pathway:

Signal transducer and activator of transcription (STAT) are a group of proteins which play roles as signaling proteins as well as transcription factors and have implications in cancer progression (Yu and Jove, 2004). This family of proteins is made up of seven members: STAT1-4, STAT5a-5b, and STAT6. The STAT proteins work in tandem with Janus kinases (JAK) where JAKs become activated through interaction with an activated membrane receptor and dimerization/ transphosphorylation occurs (Rawlings et al., 2004). The activated JAKs then phosphorylate STAT proteins which then translocate to the nucleus to alter gene transcription (Rawlings et al., 2004).

STAT3 activation can occur through interleukin-6 (IL6), JAKs as described above or through interactions with Src kinases (Subramaniam et al., 2013).The activation of STAT3 lead to the activation of genes associated with increased cell proliferation, cell survival, invasion, angiogenesis and metastasis (Al Zaid Siddiquee and Turkson, 2008). STAT 3 is phosphorylated and activated at two sites, tyrosine 705 and serine 727. The activation site of STAT3 tyrosine 705 is phosphorylated through the JAKs and the kinases that phosphorylate serine 727 have yet to be determined. The phosphorylation of tyrosine 705 has been associated with poor prognosis and poor overall survival in pancreatic ductal carcinoma (Denley et al., 2013).

1.6.3 c-Jun and c-Jun N Terminal kinases (JNKs):

c-Jun is transcription factor found in the nucleus who play a role in cell proliferation, and apoptosis (Leppa and Bohmann, 1999). This transcription factor has been shown to have effects on cell proliferation in chicken embryo fibroblasts where the overexpression of c-Jun and also that removing the first 27 amino acids towards the N-terminus of c-Jun further activate its oncogenic potential (Bos et al., 1990). Post translational modifications activate c-Jun with phosphorylation sites on serine 63 and 73. c-Jun N terminal kinases (JNKs) which are thought to play roles in inflammation, cell differentiation and apoptosis, are responsible for phosphorylating these serine

residues and activating c-Jun (Karin, 1995; Weston and Davis, 2002). JNKs, also have been found to have an impact on cell migration and invasion in human adenocarcinomas (Hauck et al., 2001).A study performed in 2012 by Zhou et al. revealed the relationship between JNK/ c-Jun and FRK in glioblastoma (Zhou et al., 2012). FRK is lost in high grade glioblastoma, however the reintroduction of FRK resulted in reduced signaling through JNK/ c-Jun and reduced migration and proliferation (Zhou et al., 2012).

1.6.4 PI3K/ AKT Signaling:

Phosphoinositide 3-kinases (PI3Ks) are a group of lipid bound enzymes activated through EGFR pathways and are capable of phosphorylating 3' OH of phosphoinositol to phosphatidylinositol 3, 4, 5-triphosphate (PIP_3) in response to extracellular signals (Kaplan et al., 1987). Phosphorylation of PIP_3 results in a cellular message that impacts cell growth, cell survival, and cell proliferation but this phosphorylation event can be reversed by PTEN (Bader et al., 2005; Maehama and Dixon, 1998). AKT is a protein kinase that is responsible for mediation of signals from the second messenger PIP_3 and generally found to be hyper active in tumors (Cantley, 2002). PIP_3 allows for AKT to bind through its pleckstrin homology domain (PH domain) localizing to the membrane where it can interact with its many substrates that result in cell proliferation, and cell survival (Manning and Cantley, 2007).

Table 1

FRK cancer associated mutations found utilizing cBioPortal. Mutations listed include nonsense, frameshift, in-frame deletion, in-frame deletion+insertion and missense mutations. Some of these include activating FRK mutants in liver cancer (20-31) (Goel and Lukong, 2016).

S. no.	Patient tissue/cell line designation	Amino acid mutation	Mutation type	Designated cancer study
1.	*TCGA-43-6647-01*	S184X	Nonsense	Lung squ. (TCGA pub.)
2.	*TCGA-39-5016-01*	R179X	Nonsense	Lung squ. (TCGA pub.)
3.	*TCGA-D1-A103-01*	K149X	Nonsense	Uterine (TCGA)
4.	*TCGA-FU-A3HZ-01*	E151X	Nonsense	Cervical (TCGA)
5.	Kuramochi_Ovary	R64X	Nonsense	CCLE (Novartis/Broad 2012)
6.	NCIH 2342_Lung	E146X	Nonsense	CCLE (Novartis/Broad 2012)
7.	NCIH 2126_Lung	Y193X	Nonsense	CCLE (Novartis/Broad 2012)
8.	CW-2_colon	G341E fs*30	Frame-shift	CCLE (Novartis/Broad 2012)
9.	TT_thyroid	S184N fs*14	Frame-shift	CCLE (Novartis/Broad 2012)
10.	*TCGA-32-2638-01*	V370	Frame-shift	GBM (TCGA 2013)
11.	*Pfg068T*	Y151I fs*14	Frame-shift	Stomach (Pfizer_UHK)
12.	*TCGA-F1-6177-01*	Y151N fs*7	Frame-shift	Stomach (TCGA pub.)
13.	*TCGA-F1-6177-01*	G150E fs*8	Frame-shift	Stomach (TCGA)
14.	*LUAD-NYU669*	L177S fs*22	Frame-shift	Lung Adeno. (Broad)
15.	*TCGA-05-4249-01*	R181del.	In-frame del.	Lung Adeno. (TCGA)
16.	MDA_N	*X211*	Splice	NCI-60
17.	MDA-MB-435	*X*211	Splice	NCI-60
18.	CW-2_colon	*X*267	Splice	CCLE (Novartis/Broad 2012)
19.	*17330*	*X*320	Splice	Lung Adeno. (TSP)
20.	*CHC341T_Liver*	E346G	Missense	Pilati *et al.*, Cancer Cell, 2014
21	*CHC544T_Liver*	*V378-F379del.*	In-frame del.	Pilati *et al.*, Cancer Cell, 2014
22.	*CHC624T_Liver*	*V378–K380del.E*	In-frame del.+ins.	Pilati *et al.*, Cancer Cell, 2014
23.	*CHC627T_Liver*	*F379-K380del.L*	In-frame del.+ins.	Pilati *et al.*, Cancer Cell, 2014
24.	*CHC970_Liver*	*V378-F379del.*	In-frame del.	Pilati *et al.*, Cancer Cell, 2014
25.	*CHC1130T_Liver*	E346G+Y350C	Missense	Pilati *et al.*, Cancer Cell, 2014
26.	*CHC1239T_Liver*	E346G	Missense	Pilati *et al.*, Cancer Cell, 2014
27.	*CHC1240T_Liver*	*V378-F379del.*	In-frame del.	Pilati *et al.*, Cancer Cell, 2014
28.	*CHC1263T_Liver*	V378del.KLN	In-frame del.+ins.	Pilati *et al.*, Cancer Cell, 2014
29.	*CHC1488T_Liver*	*V378-F379del.*	In-frame del.	Pilati *et al.*, Cancer Cell, 2014
30.	*CHC1489T_Liver*	*V378-K390del.E*	In-frame del.+ins.	Pilati *et al.*, Cancer Cell, 2014
31.	*CHC1496T_Liver*	E346G	Missense	Pilati *et al.*, Cancer Cell, 2014
32.	*TCGA-25-1326-01*	S145R	Missense	Ovarian (TCGA pub.)
33.	*TCGA-AA-A00N-01*	I4T	Missense	Colorectal (TCGA pub.)
34.	*SA106*	K265R	Missense	Breast (BCCRC)
35.	*TCGA-BT-A0YX-01*	E392K	Missense	Bladder (TCGA pub.)
36.	TCGA-HT-7481-01	A335V	Missense	Glioma (TCGA)

2.0 Rationale

BRK and FRK exhibit nearly 45% amino acid sequence homology. A recent study identified key amino acid residues in the BRK SH3, SH2, and the kinase domain which were found mutated in various cancer types (Tsui and Miller, 2015). These mutations were found to alter the enzymatic activity of BRK (Tsui and Miller, 2015). Interestingly we noted that several of these amino acid residues are conserved in FRK (**Table 2**).

Table 2.1

Cancer-related BRK mutations studied by Tsui and Miller. The type of cancer each mutant is associated with is presented and the similar amino acid in FRK.

Mutant no.	Mutation in BRK	Cancer Type	Similar residues in FRK
1	L16F	Clear cell renal cell carcinoma	L50
2	R131L	Gastric cancer	R169
3	V253M	Head and neck squamous cell carcinoma	V295
4	N317S	Ovarian Carcinoma	N359
5	L343F	Cutaneous squamous cell carcinoma	Not conserved (E388)
6	P450L	Pancreatic cancer	Not conserved (A500)

Table 2.2

Cancer-related FRK mutations presented with the cancer they were identified in.

Mutant no.	Mutation in FRK	Cancer Type
1	R64P	Breast Cancer
2	K87N	Large Intestine Cancer
3	S145R	Ovarian Cancer
4	K265R	Breast Cancer
5	N359I	Liver Cancer
6	del VF	Liver Cancer

3.0 Hypothesis

We hypothesize that mutating these conserved amino acid residues in FRK (Table 2) would alter the enzymatic activity of FRK in a manner similar to that observed in BRK. Given that FRK plays a tumor suppressor role in breast cancer, we further hypothesize that FRK cancer-associated mutations (**Table 2.2**) would alter the growth-inhibitory functions of FRK in a kinase-dependent manner.

3.1 Objectives

We propose to investigate the following specific objectives:

1. To generate point mutations in FRK and assess the effect of these mutations on FRK kinase activity.
2. To examine the effect of specific FRK SH3 and SH2 mutations on intramolecular and intermolecular interactions.
3. To assess the effect of these mutations on FRK-regulated signaling pathways JAK/STAT, AKT, and JNK/c-Jun pathways.
4. To study the effect of these mutations on FRK-regulated growth inhibition in breast cancer and liver cancer cells.

4.0 Materials and Methods

4.1 List of Reagents

Table 4.1.1

All Materials used.

Name	Manufacturer	Catalogue Number
Acrylamide	Sigma	A5934
Acetic Acid	Fisher	A465250
Agar	Fisher	BP1425-2
Agarose	Fisher	BP1360
Ammonium Persulfate (APS)	Sigma	A3678
Ampicilin	Amresco	0339-25g
Aprotinin	Sigma	A6279-10 mL
Bisacrylamide N'N-methylene	Amresco	172
Bovine Calf Serum	Thermo Scientific	SH30087.02
Chloramphenicol	Fisher	Bp904-100
Coomassie stain	Biorad	161-0406
Disodium Phosphate (NA2HPO4)	Fisher	S375-500
Dimethyl Sulfoxide (DMSO)	Fisher	TS-20684
DTT	Fisher	Bp172-25
Dulbecco's Modified Eagle Medium (DMEM)	Thermo Scientific	SH30023.01
EDTA	Fisher	Bp120-500
Fetal Bovine Serum	Fisher	10437028
GST Binding Resin	Novagen	70541-3
Gel Red	Biotium	41002
Glycerol	Sigma	G5516
Glycine	Fisher	S80028
Hydrochloric Acid (HCl)	Fisher	A508-P500
IPTG	Bioshop	IPT001.10
Kanamycin	Millipore	420311
LB Media	Fisher	Bp1426-2

Name	Manufacturer	Catalogue Number
Laemmli 2X	Sigma	1001698428
Methanol	Millipore	MX0475
Monopotassium Phosphate (KH2PO4)	Fisher	BP-362-500
NaCl	Amresco	0241-5kg
Nitrocellulose Membrane	Pall Life	66489
Phusion Polymerase	Thermo Scientific	F-530S
Potassium Chloride	Fisher	AC193780000
Polyethyleneimine (PEI)	Sigma	408727
Phenylmethylsulfonylfluoride (PMSF)	Omnipur	711OCN
Sodium Dodecyl Sulfate (SDS)	Sigma	L3771
Skim Milk	BD Difco	DF0032173
TEMED	Amresco	0761-CA-100 mL
Tris Base	Fisher	Bp152-5
Triton 100X	Sigma	T8787-100 mL
Tween	Fisher	BP337500

4.2 Identification of Cancer-Associated Mutations

4.2.1 Catalogue of Somatic Mutations in Cancer

All cancer associated mutations were found using COSMIC (Catalogue of Somatic Mutations in Cancer). COSMIC labels all mutations known onto a schematic of the protein where they can be selected in order to present information about the mutation. The information includes the tissue type the mutation is associated with, the number of times the mutation has been observed and patient information.

4.2.2 Mutation Criteria

158 mutations can currently be found for FRK on COSMIC so, in order to select a reasonable number of mutations for study we needed a criteria to avoid selecting mutations that would either have no effect on the functionality of FRK and such that we can hypothesize the reason for malfunction of FRK. The first requirment for mutations was that at least one mutation should be found in each functional domain. Secondly, mutations should be associated with breast cancer or

liver cancer as FRK has been shown to function as a candidate tumor suppressor in breast cancer and to have possible oncogenic function in liver cancer. Several muations selected occur in breast cancer or liver cancer, those being R64P, and K265R in breast cancer and N359I, and VF in liver cancer. Third, mutations that occur in coinserved motifs or adjacent to critical amino acids should be selected. Select mutations were found in conserved motifs or near critical residues, those being, S145R found in the phosphotyrosine binding pocket, N359I found in the DLAARN motif and K265R which is near the ATP contacting lysine K262. Lastly we selected mutations which have occurred more than once, those being K87N which has been seen twice, and N359I which has been seen three times.

4.2.3 Multiple Sequence Alignment

A multiple sequence alignment was performed by uploading sequences to Clustal omega in order to observe conserved regions and critical residues between FRK, BRK and SRMS. This was important for determining hypotheses for how certain mutations function.

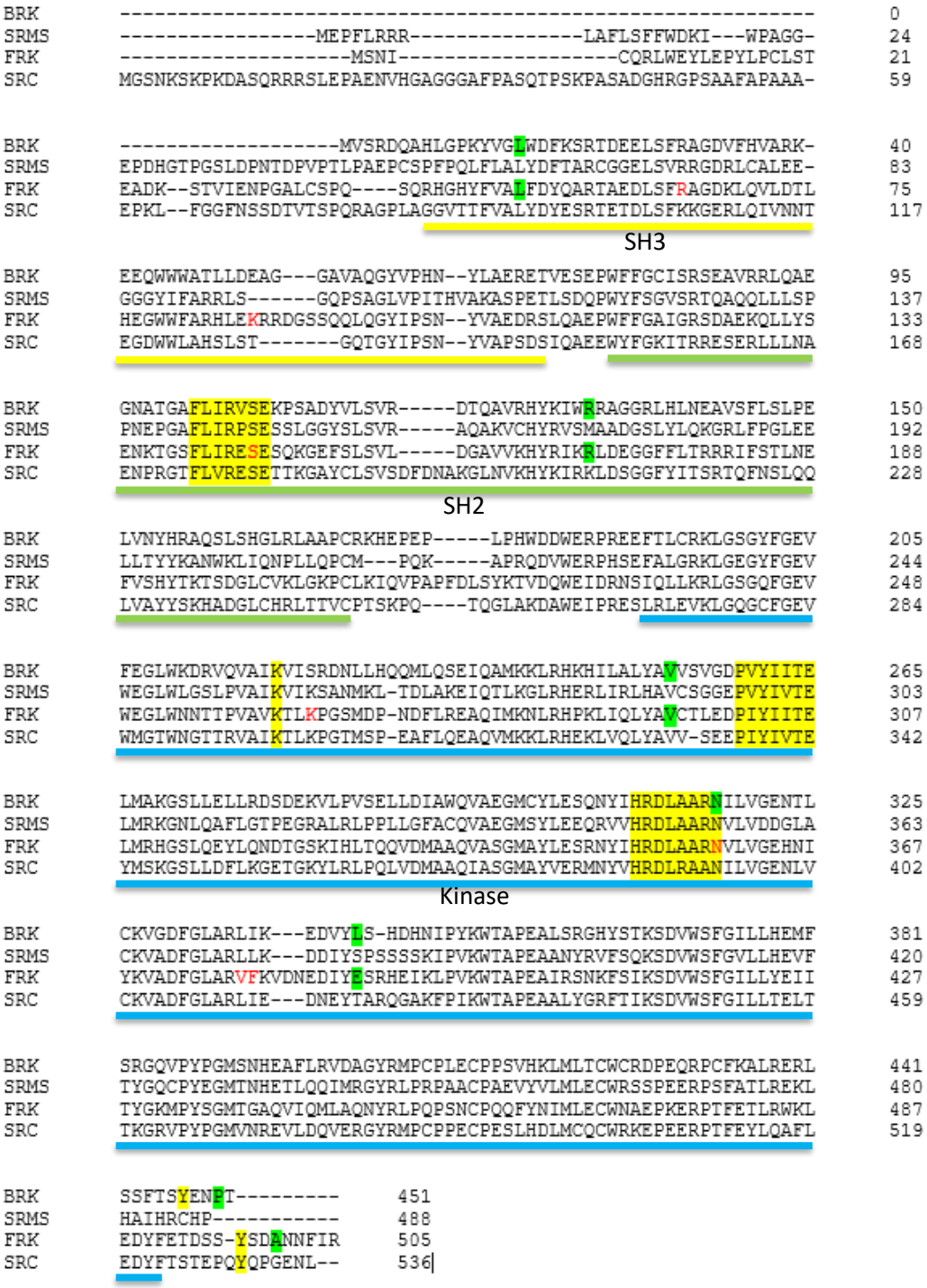

Figure 4.2 1

Multiple Sequence Alignment of FRK, BRK, SRMS, and Src. Red residues indicate FRK cancer-associated mutations**.** Green amino acids indicate cancer-associated mutations of BRK and conserved residues in FRK. Yellow highlighted residues indicate conserved regions between all proteins. SH3 (yellow), SH2 (green), and kinase (blue) domains are underlined and labelled.

4.3.0 Site Directed Mutagenesis

All PCR amplifications were performed using the Phusion polymerase (F-530S, ThermoFisher Inc, USA) supplied as a mastermix, using the manufacturer's instructions, as appended below:

PCR using *Phusion* Polymerase:

25 μL Phusion master mix, 1μL forward primer (10 μM), 1 μL reverse primer (10μM), 1 μL DMSO, 22 μL H_2O.

Cycling conditions:

1. Initial Denaturation — 98 ^oC (30 seconds)
2. Extension (30 cycles) — 98 ^oC (10 seconds)
   3 ^oC above primer melting temperatures (1 minute)
   72^oC (4 minutes)
3. Final Extension — 72^oC (5 minutes)

All mutants were transformed into the XL Gold E. *coli* cell line.

4.3.1 Primer Design

Primers were designed by analyzing the DNA sequence surrounding the point mutation. The codon of interest was exchanged for the codon of the specific mutation. 15 nucleotides on either side of the mutation were added to the primer to give the primer a length of 33 nucleotides.4.3.2 Primers

Table 4.3.2

All primers used. All written 5`-3`.

Mutation	Direction	Sequence
BRK L16F	Forward	CCCAAGTATGTGGGCTTTTGGGACTTCAAGTCC
	Reverse	GGACTTGAAGTCCCAAAAGCCCACATACTTGGG
BRK R131L	Forward	CACTACAAGATCTGGCTTCGTGCCGGGGGCCGG
	Reverse	CCGGCCCCCGGCACGAAGCCAGATCTTGTAGTG
BRK V253M	Forward	CTGGCGCTGTACGCCATGGTGTCCGTGGGGGAC
	Reverse	GTCCCCCACGGACACCATGGCCTACAGCGCCAG
BRK N317S	Forward	GACCTGGCCGCCAGGTCTATCCTCGTCGGGGAA
	Reverse	TTCCCCGACGAGGATAGACCTGGCGGCCAGGTC
BRK L343F	Forward	AAGGAGGACGTCTACTTTTCCCATGACCACAAT
	Reverse	ATTGTGGTCATGGGAAAAGTAGACGTCCTCCTT
BRK P450L	Forward	ACCAGCTACGAGAACCTTACCTGA
	Reverse	TCAGGTAAGGTTCTCGTAGCTGGT
FRK L50F	Forward	CACTACTTTGTGGCTTTTTTTGATTACCAGGCT
	Reverse	AGCCTGGTAAAAAAAAGCCACAAAGTAGTG
FRK R169L	Forward	CACTACAGAATTAAACTACTGGATGAAGGGGGA
	Reverse	TCCCCCTTCATCCAGTAGTTTAATTCTGTAGTG
FRK V295M	Forward	ATCCAGCTTTATGCTATGTGCACTTTAGAAGAT
	Reverse	ATCTTCTAAAGTGCACATAGCATAAAGCTGGAT
FRK N359I	Forward	GATCTGGCTGCCAGAATTGTCCTCGTTGGTGAA
	Reverse	TTCACCGAGGACAATTCTGGCAGCCAGATC
FRK E388I	Forward	AATGAAGACATCTATATTTCTAGACACGAAATA
	Reverse	TATTTCGTGTCTAGATAAATAGATGTCTTCATT
FRK A500W	Forward	TCTTCATATTCAGATTGGAATAACTTCATAAGA
	Reverse	TCTTATGAAGTTATTACCATCTGAATATGAAGA
FRK R64P	Forward	GAGGACTTGAGCTTCCCTGCAGGTGACAAACTT
	Reverse	AAGTTTGTCACCTGCAGGGAAGCTCAAGTCCTC
FRK K87N	Forward	GCCAGACACTTGGAGAATAGACGAGATGGCTCC
	Reverse	GGAGCCATCTCGTCTATTCTCCAAGTGTCTGGC
FRK K265R	Forward	GCAGTGAAAACATTACGTCCAGGTTCAATGGAT
	Reverse	ATCCATTGAACCTGGACGTAATGTTTTCACTGC
FRK VF	Forward	TTTGGACTTGCCAGAAAGGTAGATAATGAA
	Reverse	TTCATTATCTACCTTTTCTGGCAAGTCCAAA

4.4 Transformation

The PCR product was treated with 1 μL of Dpn I overnight in order to degrade the parental plasmid. Competent XL Gold cells were used for the transformation which were thawed for 15 minutes. Then 5 μL of the PCR product was added to 50 μL of the competent cells. This was allowed in incubate on ice for 30 minutes. The cells were heat shocked at 42^{o}C for 1 min and placed back on ice for four minutes. 300 μL of antibiotic free media was added and was incubated at 37^{o}C in a shaker for one hour. The cells were then centrifuged at 1000 x g for 1 min and resuspended in 80 μL of antibiotic free media. The entire contents were then spread on an agar plate with appropriate antibiotic drug and incubated for 12 – 16 hours. Colonies were picked using pipette tips and grown in 5 mL cultures with the appropriate antibiotic for 12 hours.

4.4.1 DNA Isolation for Transformation (Mini/ Maxi Prep)

4.4.1.1 Mini Prep: Small Scale DNA Isolation

1.5 mL of culture was taken and centrifuged at 5000 x g for one minute. The cell pellet was resuspended in 110 μL of P1 buffer (Qiagen). Once resuspended, 100 μL of P2 lysis buffer (Qiagen) was added and incubated for four minutes at room temperature. Immediately after the four-minute incubation, 120 μL of P3 neutralization buffer (Qiagen) was added and the tubes were shaken vigorously until a white precipitate had formed. This was centrifuged at 17000 x g for 10 minutes and the supernatant was transferred to a new tube where the DNA was precipitated with 200 μL of cold isopropanol. The DNA was centrifuged at 17000 x g for one minute and the supernatant removed. 500 μL of 70% ethanol was added to the DNA pellet and centrifuged at 17000 x g for one minute. The ethanol was poured off and the DNA was centrifuged at 17000 x g for one minute. At which point the remaining ethanol was removed using a pipette and the DNA pellet was allowed to air dry for 15 minutes. Once dry the DNA pellet was resuspended with 30 μL of ddH20 and quantified using nanodrop. DNA from this process was used mainly for transformation.

4.4.1.2. Maxi Prep:

500 mL of starter culture was added to 400 mL of media with appropriated antibiotic and incubated for 12-16 hours. The culture was centrifuged at 5000 x g for 10 minutes and the pellet was resuspended in 10 mL of P1 buffer (Qiagen). 10 mL of P2 lysis buffer (Qiagen) was added and incubated for four minutes, at which point 10 mL of P3 neutralization buffer was added and shaken until a white precipitate had formed. This then incubated on ice for 20 minutes and was then centrifuged at 20000 x g for 30 minutes. DNA binding column Qiagen-tip 500 (Qiagen) was equilibrated with 10 mL of QBT buffer (Qiagen) and allowed to empty by gravity flow. The supernatant containing plasmid DNA was then added to the column and emptied through gravity flow. The column was then washed with 2 times with 30 mL of QC buffer (Qiagen). DNA was then eluted with 15 mL of QF buffer (Qiagen) into a tube containing 10.5 mL of cold isopropanol. Precipitated DNA was then centrifuged at 17000 x g for 10 minutes and the supernatant discarded. DNA pellet was then washed using 5 mL of 70% ethanol and centrifuged at 17000 x g for 10 minutes. Supernatant was removed again, and the DNA pellet was centrifuged at 17000 x g for an additional 10 minutes. DNA was allowed to air dry for 15 minutes where it was resuspended in 300 μL of TE buffer and quantified using nanodrop. DNA from this process was used mainly for transfection.

4.4.2 DNA Sequencing:

DNA to be sequenced was diluted to 100 ng/ mL in a 10 μL volume and primers located 400-500 bp upstream of were diluted to 50 μM in a 50 μL volume. Sanger sequencing was performed at the NRC and analysis was performed utilizing pDraw software.

4.5 Cell Culture:

All cell lines were maintained in high glucose (4.5 g/L) Dulbecco's modified eagle media (DMEM) with 10% bovine calf serum (BCS). Wastes comprising of cells, trypsin and other components was disposed of with 30% bleach and sent in double sealed bags for autoclaving and were further disposed of. All working utensils and latex gloves were decontaminated with a thorough spraying of 70% ethanol before use.

4.5.1Cell Lines Used:

Cell lines used included, HEK293, MDA-MB-231, and HEP3B. HEK293 and HEP3B were supplemented with 10% bovine calf serum, where MDA-MB-231 was supplemented with 10% fetal bovine serum (FBS).

4.5.2 Plasmids Used:

Plasmids used were pE-GFP for transient transfection, LPC for stable cell line generation, and PRL-652 for bacterial protein expression.

4.6 Transfection

HEK 293 cells were transfected when the plate was 70% full at which point 2.5 μg of DNA was combined with 110 μL and of 150 mM NaCl. 15 μL of 1% PEI (polyethylene imine) (Sigma Aldrich) was added and incubated for 10 minutes at room temperature. The entire contents were then added dropwise to the cells. Cells were allowed to incubate for 24 hours and were assessed for fluorescence.

4.6.1Cell Lysate Preparation:

Cells after transfection or from stable cell lines were lysed around 90-95% confluent in six-well plates. Media was removed from wells and 200 μL of 2X laemmli buffer was added to each well. The cells and buffer were scraped until the entire well had been covered and the buffer had become viscous. Buffer and cells were then pipetted into a new tube and were boiled at 100^{o}C for 5 minutes.

4.7 Western Blotting

The transfection efficiency was estimated 24 hours after transfection. Cells were then lysed in 200 μL of 2X Laemmli. The samples were boiled for 5 minutes and 5 μL was loaded on a 10% polyacrylamide gel. The gel was resolved for 1 hour at 100V. All proteins were transferred to a membrane by pressing the gel to the membrane in between sheets of filter paper and resolved for 1.5 hours at 100V. The membrane was blocked for 40 minutes with skim milk (5%). Following blocking, the primary antibody (anti phospho- tyrosine, and anti GFP, 1:1000) was added and incubated on a shaker at 4^{o}C overnight. The membrane was washed 3 times with 1X PBST for 5

minutes. Secondary antibody solution was added to the membrane and incubated at 1.5 hours at room temperature. The membrane was washed with PBST, similarly to the previously stated method. Antibodies that bound the GST fusion protein were visualized on licor.

4.8 Stable Cell Line Generation

The amphotrophic HEK 293T cell line was utilized for generation of FRK containing retrovirus. The FRK LPC vector was transfected into the amphotrophic cell line when the cells covered 70% of the plate at which point 12.5 μg of DNA was combined with 550 μL of 150 mM NaCl and 15 μL of 1% PEI (polyethylene imine) and incubated for 10 minutes at room temperature. The entire contents were then added dropwise to the cells. The virus is released into the media and harvested 24 and 48 hours after transfection. Each collected volume of virus is used to transduce MDA-MB-23. Puromycin was then added at a concentration of 2.5 μg/ mL to select for transduced cells. Selection continued until colonies had formed. Polyclonal populations were selected for further experimentation.

4.9 Cloning

4.9.1. Cloning into pRL-652

Mutagenesis was performed as previously described in section 4.2 on existing FRK WT SH3 and SH3 domains in the PRL-652 vector

4.9.2Cloning into LPC vector

Mutagenesis was performed as previously described section 4.2 on existing FRK WT full length DNA in the LPC vector.

4.10 Polyacrylamide Gel:

Resolving gel: Acrylamide (10%), Tris pH 8.8 (375 mM), SDS (0.1%), APS (0.1%), TEMED (0.01%), H_2O up to 8 mL.

Stacking gel: Acrylamide (6%), Tris pH 6.8 (125 mM), SDS (0.1%), APS (0.1%), TEMED (0.01%).

Both gels were allowed to solidify for 15 to 20 minutes before proceeding.

4.11 Migration Assay

Cell migration was analyzed using a wound healing assay. Approximately 200 000 cells were added to each well of a 12 well plate and allowed to incubate for 12 hours. Once all the cells had adhered to the surface, a 200 μL pipette tip was used create a wound down the center of the plate. The closure of each wound was monitored every 12 hours by measuring the area within the wound using imageJ. The cells were monitored for three days to assess the closure of the wound.

4.12 Proliferation Assay

Cell proliferation was analyzed by measuring mitochondrial viability using Cell Counting Kit-8 (CCK-8) (Dojindo, CK04-05). The CCK8 compound was reduced by mitochondrial dehydrogenases. This reduction causes the compound to change colour based on the number of viable cells present. 1000 stable cells were seeded in 96-well plates and cultured in 100 μL culture medium (1000 cells/well). The cell proliferation assay was performed for 5 days. 10 μL of CCK-8 solution was added to each well, and then the cells were incubated for 2 hours at 37^{o}C. Following treatment with CCK-8, absorbance was read at 450 nM.

4.13 Invasion Assay

Cell invasion assay was performed using EMD Millipore Boyden chambers including a polycarbonate 8.0 μm pore size coated with extracellular matrix (EMD Millipore ECM550) following the manufacturer's instructions with slight modifications. Boyden chambers were allowed to reach room temperature and 200 μL of DMEM media lacking FBS was added for two hours to rehydrate the membrane. Cells were counted and resuspended ($2x10^5$ cells/ well) in serum free media and added to the inserts. Each insert was placed in a well of a 24 well plate containing 500 μL of 10% FBS DMEM media and incubated for two days at 37^{o}C. Following incubation, the media on the interior of the chamber was removed and the insert was placed in 500 μL of trypan blue stain for 20 minutes. Excess dye was removed, and cells were counted.

4.14 Rotational Anisotropy

Rotational anisotropy was used the measure the binding affinity of the SH3 and SH2 domains and their mutants to fluorocein labeled peptides. The reactions were 60 μL and contained a fluorocein labeled peptide at a concentration of 50 nM in buffer (1 mM DTT, 50 mM Tris, 150 mM NaCl)

and the FRK domain was titrated in at varying concentrations depending on the experiment until saturation occurred. The equipment used to collect data and calculate anisotropy was a QuantaMaster QM-4 spectrofluorometer (Photon Technology International) with a dual emission channel. The samples were excited with vertically polarized light at 495 nm and vertical and horizontal emissions were measured at 520 nm. Dissociation constants (K_d) were found by fitting a sigmoidal curve using sigma plot software.

4.14.1 Protein Purification

E.coli containing the bacterial expression vector with the FRK mutants were grown in a 5 mL culture with 5 μg/ mL ampicillin. The culture was grown for 12-16 hours and then transferred to 1 L of LB media and grown for 3-5 hours or until the OD_{600} = 0.6-0.8 (optical density at 600 nm). Protein expression was then induced with 1 mM (final concentration) IPTG and the culture was incubated at 15^{o}C for an additional 16 hours. Cultures were then centrifuged at 5000 x g and resuspended in 20 mL of lysis buffer (1 mM DTT, 50 mM Tris, 150 mM NaCl, 1% Triton, PMSF 100 mM, Aprotinin 2 mM). The bacterial resuspension was then lysed through sonication using one second bursts, ten times, and for 5 rounds. Cell lysate was centrifuged at 20000 x g for 30 minutes and supernatant was incubated overnight at 4^{o}C on GST binding resin (Novagen, 70541) which had been equilibrated with three 5 mL washes of buffer (1 mM DTT, 50 mM Tris, 150 mM NaCl). Three 5 mL washes with buffer were done to remove any protein bound non-specifically. All GST-FRK constructs were eluted from the column using buffer with 20 mM glutathione plus 10% glycerol and aliquoted into 1 mL volumes. Each volume was then visualized via coomassie and quantified using Bradford test.

4.15 Statistics

All statistics performed were student t-tests, using the functionality of Excel.

5.0 Results

FRK and BRK mutations were generated via site directed mutagenesis and confirmed through DNA sequencing. All constructs were cloned into the pE-GFP vector to assess phospho tyrosine activity via transient expression. Mutations within the SH3 and SH2 domains (R64P, K87N, and

S145R) were cloned into the pRL-652 vector for expression in E. *coli* cells to assess the effects on binding. FRK constructs N359I, VF, R64P and K265R were cloned into the LPC vector designed for stable cell line generation. The activity of each construct was observed through transfection into HEK 293 cells and western blotting with anti-phosphotyrosine and anti-GFP antibodies. Mutations selected from breast cancer and liver cancer were stably expressed in MDA-MB-231 cells and anti-proliferative effects were assessed using proliferation, CCK8; migration, wound healing; and invasion assays, Boyden chambers.

5.1 Effect of Similar FRK Mutations on Enzyme Activity

A previous study on BRK (Tsui and Miller, 2015) characterized six cancer related mutations in BRK and it was found that these residues were similar in FRK or found adjacent to the autophosphorylation site and C-terminal regulatory tyrosine. Through the transient expression of these constructs from FRK and BRK in HEK 293 cells we observed that these conserved residues have differing functions in FRK (**Figure 5.2**).

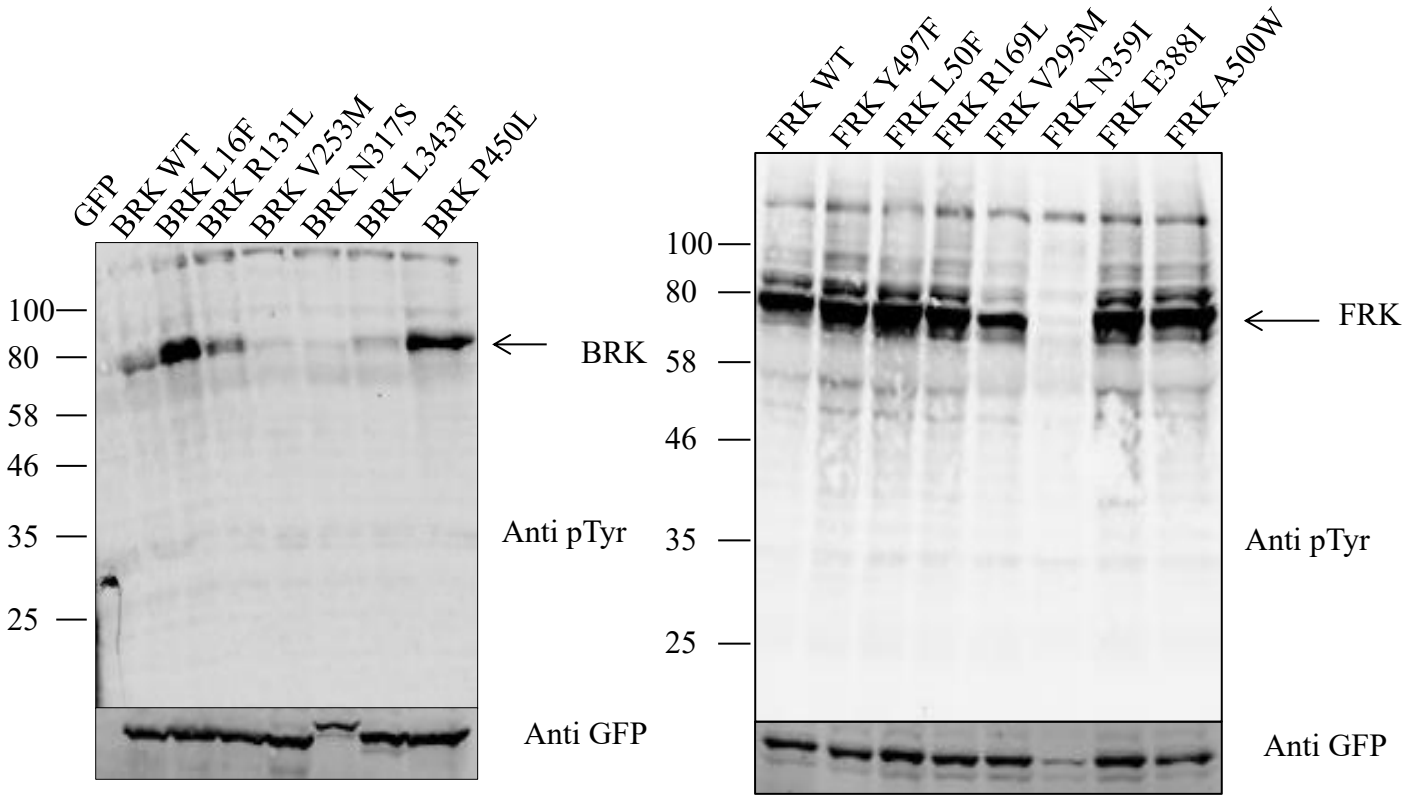

Figure 5.1

(Left) HEK 293 cells were transfected and transiently expressing BRK cancer related mutations. Global phospho-tyrosine activity analyzed through western blot utilizing phospho-tyrosine and GFP Antibodies. (Right) Transient Expression of mutated FRK residues that are similar to the BRK cancer-related mutations in HEK 293 cells. Global phospho-tyrosine activity analyzed through western blot utilizing phospho-tyrosine and GFP Antibodies

The cancer related mutations of BRK displayed varying effects on activity. Several mutations enhanced the kinase activity which include L16F and P450, whereas R131L, V253M, N317S and L343F revealed a reduction in kinase activity. When analyzing the mutation of conserved residues in FRK we found that these mutations exhibited differential phosphorylation compared to the cancer related mutations in BRK (**Figure 5.2**). All FRK mutations maintained the kinase activity

comparable to the wild type protein except for V295M and N359I which show reduced and abolished activity, respectively.

5.2 Effect of Cancer-Related FRK Mutations on Activity

A number of cancer related mutations in FRK have been catalogued in a series of databases and several mutations were chosen to analyze more in depth. All mutants were examined through western blot techniques and compared to wild type FRK which displays upregulated kinase activity. The mutations chosen for further study include R64P (Breast cancer), K87N (Large intestine cancer), S145R (Ovarian cancer), K265R (Breast cancer), N359I (Liver cancer), V378-F379 del (VF) (Liver cancer) and V378-K380 del (Liver cancer). The VF mutation was identified in a previous study (Pilati et al., 2014). The SH3 domain mutations (R64P, K87N) and the SH2 domain mutation (S145R) all showed kinase activity similar to wild type. The kinase mutation VF (V387-F379 del) showed elevated kinase activity. K262R exhibited reduced kinase activity and N359I abolished kinase activity (**Figure 5.2.1**). These were seen as statistically significant through the quantification of all activities as presented in figure 5.2.2.

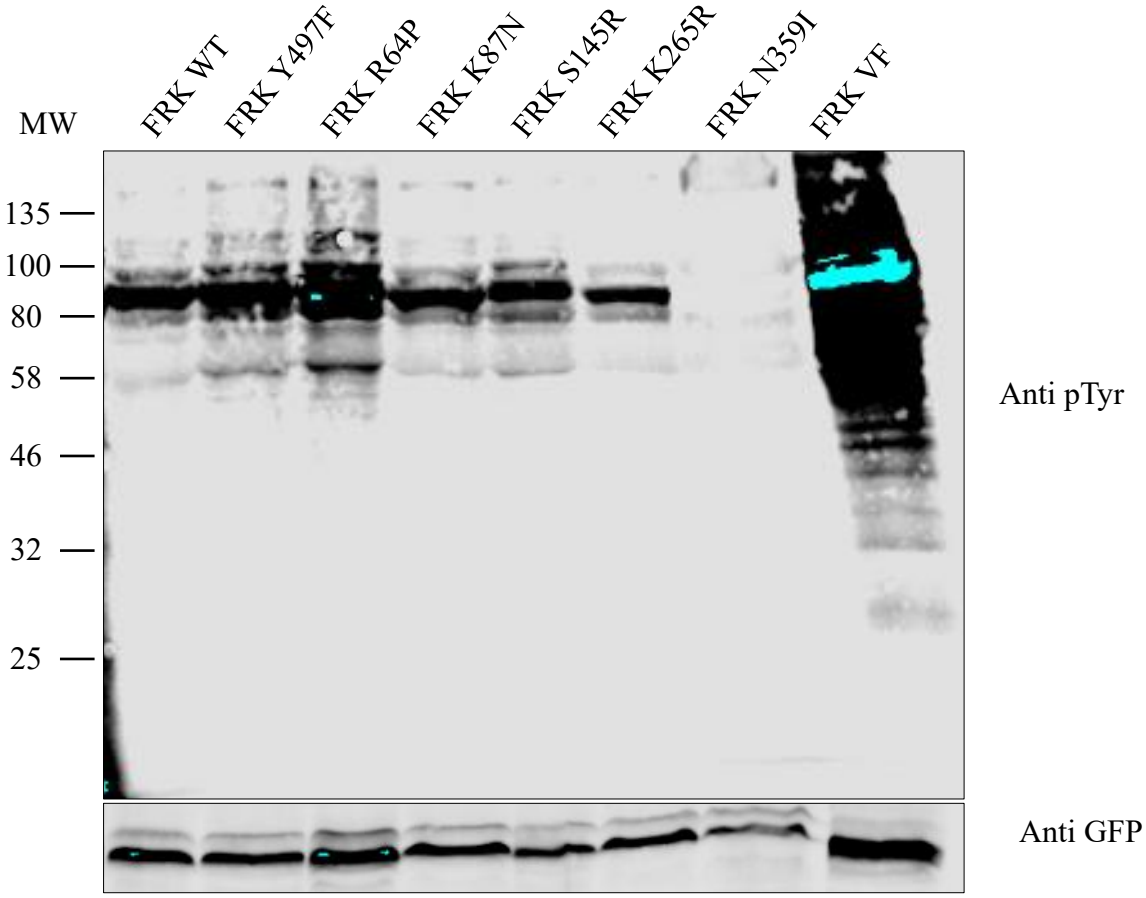

Figure 5.2.1

Transient Expression of cancer related FRK mutations in HEK 293 cells. Global phospho-tyrosine activity analyzed through western blot utilizing phospho-tyrosine and GFP Antibodies.

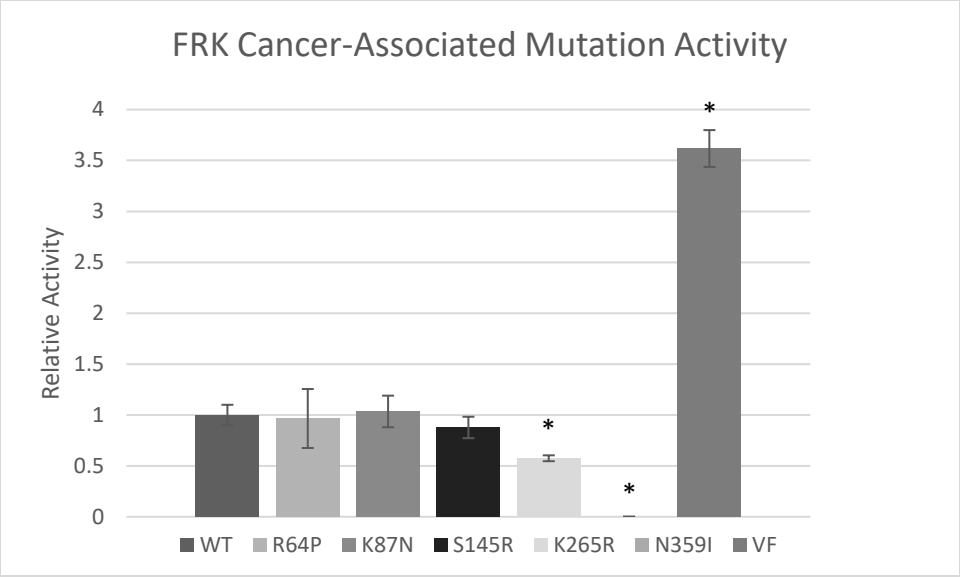

Figure 5.2.2

Kinase activity of each mutation relative to the kinase activity of wild type FRK. With significant differences being indicated by *. K265R, and N359I exhibit reduced kinase activity and VF shows elevated kinase activity.

5.3 Visualization of Cancer-Associated Mutations Located in Conserved Motifs

In order to interpret the change of level of kinase activity we used a SRC crystal structure to analyze the importance of mutations S145R and N359I using PyMOL software. Src was used because of readily available crystal structures where the conserved motifs could be viewed. The reason we were only able to analyze these two mutants is because these were the only mutations located in highly conserved motifs and the structure of FRK has not yet been solved. The first of the two mutations is the S145R mutant which lies in the phospho-tyrosine binding site within the SH2 domain. This specific serine residue has also been noted to be involved in phospho-tyrosine binding in the Abl kinase. Also the mutation of this serine in Abl kinase resulted in lost phospho-tyrosine binding (Mayer et al., 1992). We therefore expected that this mutation would disrupt the self-regulation of FRK and result in increased activity.

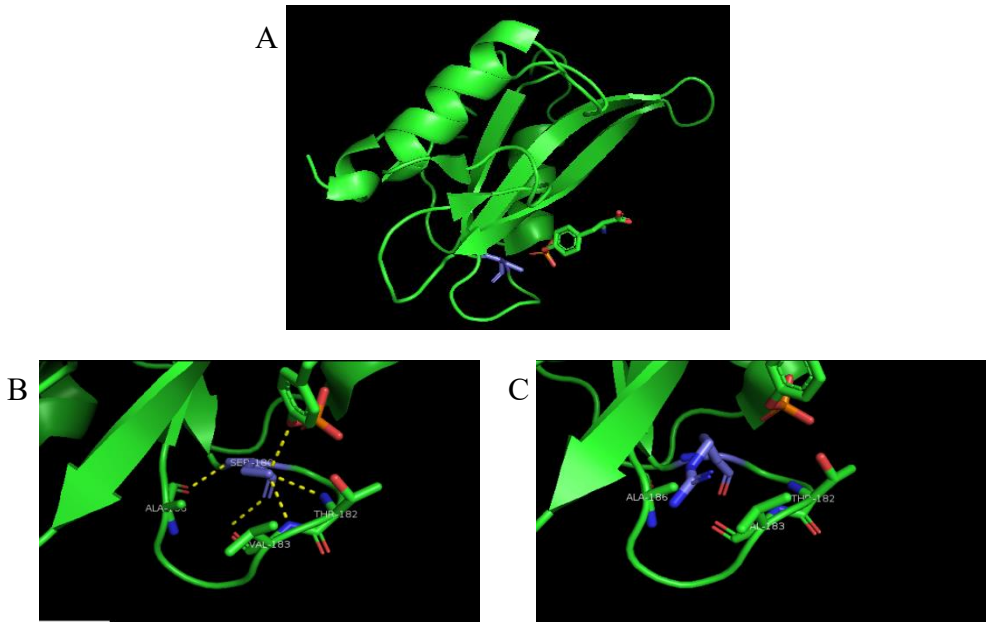

Figure 5.3.1

Mutation of S145R (FRK) shown using a SRC SH2 crystal structure 4F5B. **A)** The entire SRC SH2 domain crystal structure. **B)** Close up of the serine 180 (Blue) (SRC) exhibiting the hydrogen bonding of S180. **C)** Serine 180 (SRC) mutated to arginine mimicking the S145 in FRK

5.3.1: S145R FRK SH2 Domain

This model shows the serine interacting directly with the phospho-tyrosine as well as the backbone of residues 182 and 183 (**Figure 5.3.1**). Mutating this residue to an arginine results in a number of different rotamers and the most frequently occurring rotamer results in lost binding to the phosphor-tyrosine and lost interactions with the neighbouring residues. Mutating this serine residue in the SH2 phospho-tyrosine binding sequence should result in the lost self-regulation of FRK as well as increased kinase activity.

5.3.2: N359I FRK Kinase Domain

The second mutation visualized the (N359I) lies in the activation loop of FRK. This mutation lies in a motif is highly conserved and is found most often in NRTKs.

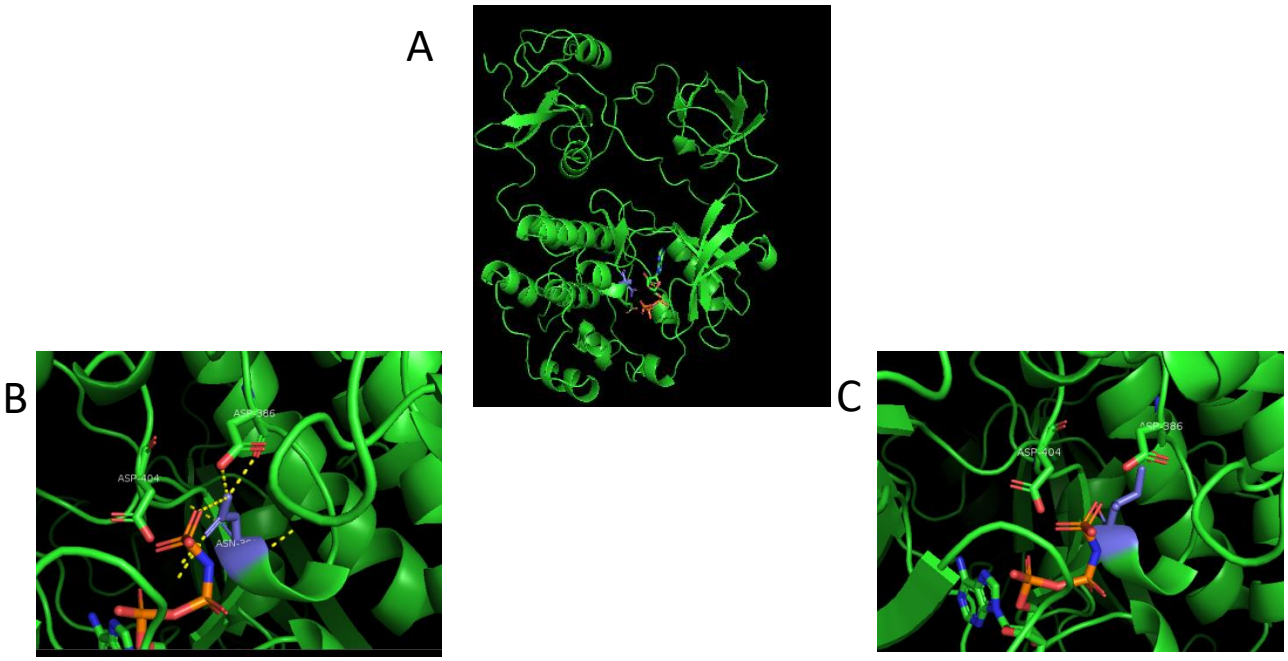

Figure 5.3.2

Mutation of N359I (FRK) shown using a SRC crystal structure 2SRC. **A)** Complete SRC crystal structure complexed with ANP-PNP (ATP analogue). **B)** Close up of N394 (Blue) (SRC) exhibiting the hydrogen bonding of N394. **C)** N394 (SRC) mutated to isoleucine mimicking the N359I (FRK).

In Figure 5.4.2, the wild type asparagine appears to be interacting with both the ATP molecule as well as aspartate 386. Aspartate 386 is known as the catalytic base that is required for the proper function of the kinase. This aspartate residue has been shown to deprotonate the tyrosine of the target protein (Cheng et al., 2010). Mutating the asparagine 386 residue to isoleucine in SRC disrupts the interaction with both the aspartate 386 and the ATP molecule. Loss of these interactions should cause decreased kinase activity due to improper ATP positioning or because aspartate 386 is no longer positioned to deprotonate the target tyrosine.

5.4 Effect of Cancer-Associated Mutations on Cell Proliferation

FRK has been previously shown to supress proliferation in MCF7 and MDA-MB-231 breast cancer cells (Ogunbolude et al., 2017b; Yim et al., 2009). In order to analyze the rate of cell growth, stable cell lines were generated using select mutations. Of the mutations that were analyzed above,

the two breast cancer mutations (R64P and K265R) and the two liver cancer mutations (N359I and VF) were stably expressed in MDA-MB-231 cells. This cell line was chosen because it shows low levels of FRK and is a highly metastatic and tumorigenic cell line. These qualities exhibited make MDA-MB-231 an ideal cell line to test the tumor suppression function of FRK.

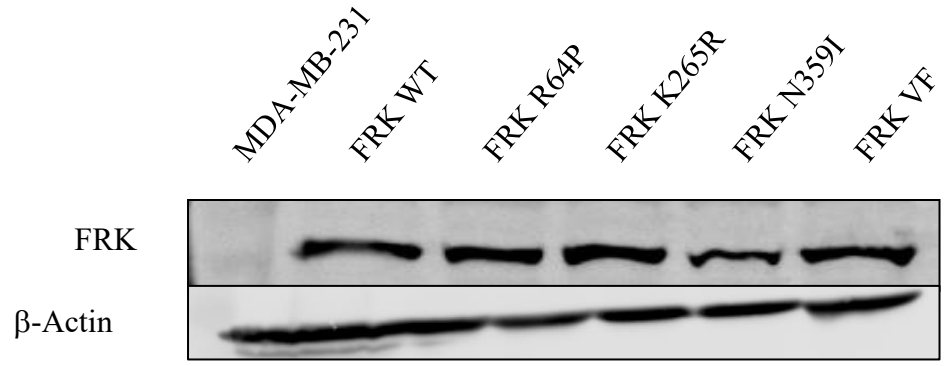

Figure 5.4.1 1

Stable expression of FRK measured using western blotting and FRK antibodies. Wild type FRK (FRK WT), FRK R64P, FRK K265R, FRK N359I, FRK VF

The control was the MDA-MB-231 cell line without exposure to the FRK containing retrovirus. All five constructs: FRK WT, FRK R64P, K265R, N359I, and VF showed significant expression of FRK after with selection with puromycin into polyclonal populations. To assess cell proliferation rates, we employed the CCK-8 reagent which measures dehydrogenase activity in active mitochondria and can be used to quantify the number of viable cells. We hypothesized that the mutants with higher kinase activity (**Figure 5.4.1**) than the wild type FRK would have more of a dramatic anti-proliferative effect where the R64P and VF mutants would have decreased proliferation, K265R and N359I would not have as drastic of an anti-proliferative effect as the wild type FRK.

FRK wild type expressing cells resulted in a significantly reduced growth rate (**Figure 5.5.2**) compared the MDA-MB-231 cell line (p value < 0.05) alone which has been shown previously by our lab (Ogunbolude et al., 2017b). The mutations tested: R64P, K265R, N359I, VF, did not result in a change in cell proliferation that was significantly different than the wild type FRK. However,

these mutations still showed a decreased proliferation rate compared to the MDA-MB-231 cell line (p value < 0.05).

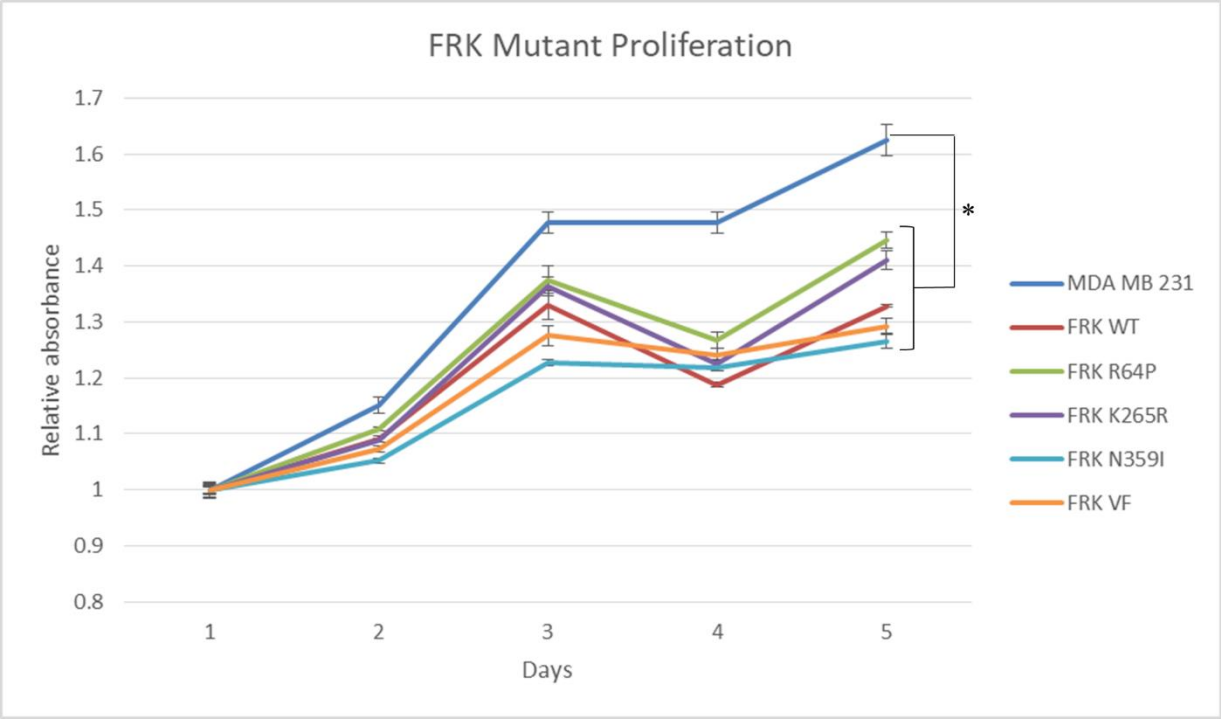

Figure 5.4.2

Cell proliferation rates of labelled FRK MDA-MB-231 cell lines measured with the CCK-8 assay. Wild type FRK (FRK WT), FRK R64P, FRK K265R, FRK N359I, FRK VF. Significantly different growth rates are indicated by *.

5.5 Cell Migration:

Our lab has also previously shown the expression of FRK in breast cancer cell lines results in reduced rates of migration, so we therefore conducted similar wound healing experiments with the above mentioned stable cell lines (Ogunbolude et al., 2017b). A vertical scratch was made using a pipette tip and the closure of the wound was monitored every 8 hours (**Figure 5.5.1**). Again, we had predicted that the rate of cell migration could be predicted by the kinase activity of each of the mutations. This would mean that the mutations with increased kinase (R64P, VF) activity would exhibit a reduced migration rate compared to the wild type FRK and the mutations with reduced kinase activity (K265R, N359I) would exhibit increased migration rates. At the 56-hour point which is the time point where the control MDA-MB-231 wound had fully closed, the wild type, R64P, K265R, N359I and VF mutations had closed to 66%, 41%, 38%, 42%, and 53%

respectively. Mutations R64P, K265R, and N359I resulted in a wound closure to between 38% and 42% which is a statistically significant increase of migration compared to the wild type FRK but decrease compared to MDA-MB-231. The VF mutation resulted in migration rate that was slower than the other mutations but not statistically different compared to the wild type FRK.

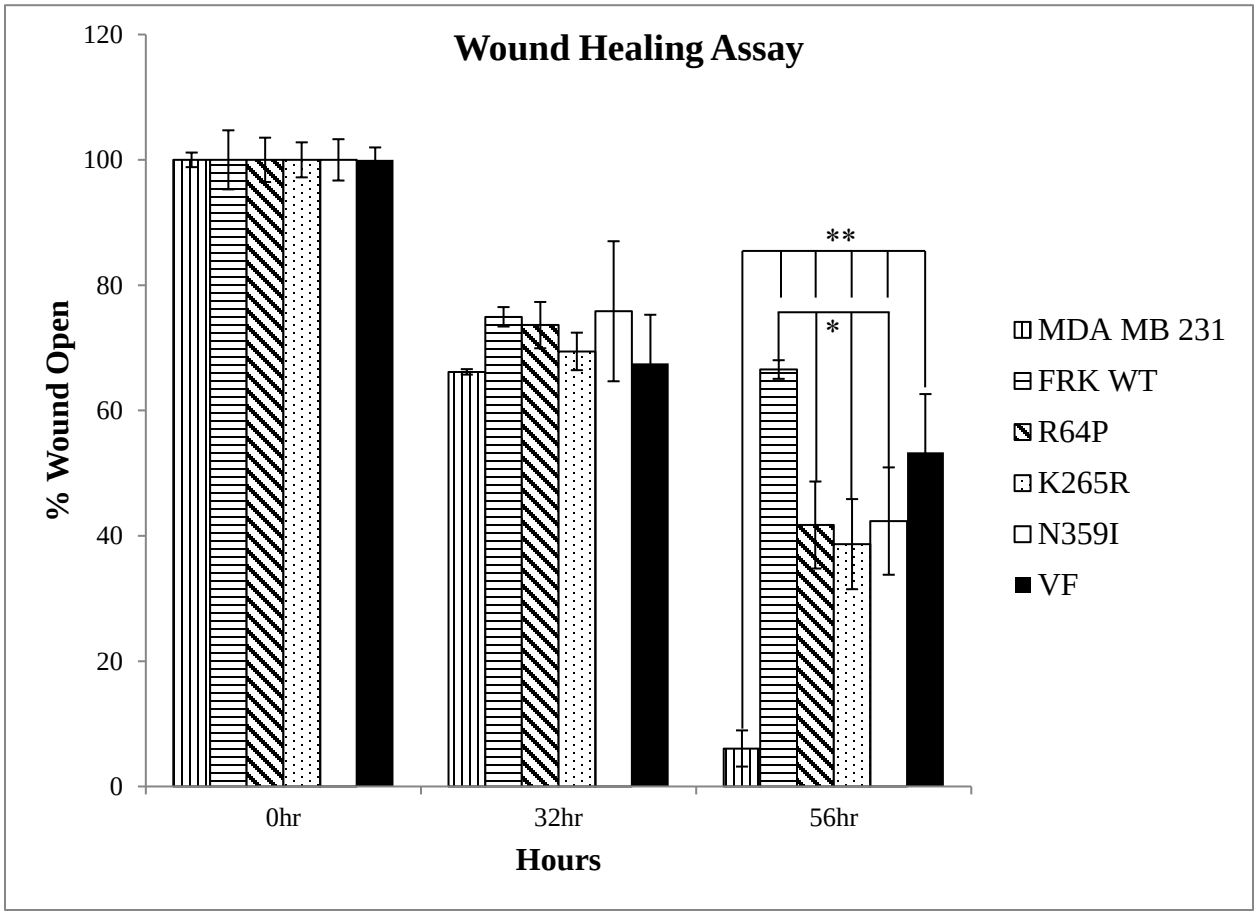

Figure 5.5.1

Cell migration of FRK stable cell lines measured using a wound healing assay. Wild type FRK (FRK WT), FRK R64P, FRK K265R, FRK N359I, FRK VF

5.6 Cell Invasion Assay:

To examine the effect of the cancer associated FRK mutations, a Boyden chamber coated with extracellular matrix was used. The data presented showed that the cell line expressing wild type FRK showed significantly reduced cell invasion ($P<0.05$; **Figure 5.6.1**) by 35%. The cancer associated mutations were found in breast and liver cancer exhibit varying degrees of activity compared to the wild type FRK all show similar levels of invasion to the MDA-MB-231 control cell line.

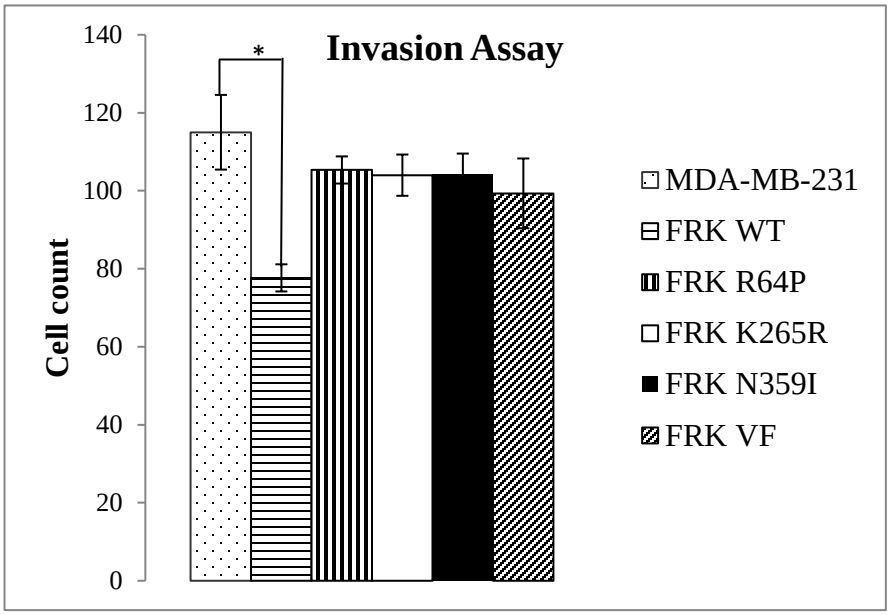

Figure 5.6

Cell invasion assay performed using Boyden chambers coated in extracellular matrix to analyze the invasive properties of the FRK stable cell lines. Wild type FRK (FRK WT), FRK R64P, FRK K265R, FRKN359I, FRK VF.

5.7 FRK Mutation effect on Signaling:

5.7.1 FRK Mutation effect on Signaling in Stable Cell Lines:

All FRK mutant stable cell lines were lysed as described above and their effect on signaling was assessed via western blotting. The signaling proteins evaluated were STAT3 and pSTAT3 on tyrosine 705, JNK and pJNK on tyrosine 185, c-Jun and p-c-Jun on serine 63, and AKT and pAKT on serine 473. FRK expression was shown to decrease levels of phosphor c-Jun and JNK (Zhou et

al., 2012), as well as a reduction in STAT3 and AKT signaling (Ogunbolude et al., 2017). However, when analyzing the effect present within the stable cell lines expressing FRK WT and cancer associated mutations, little effect was seen on any of the signaling molecules mentioned above as shown in figure 5.7.1. The only effect noted was a slight reduction in phospho-c-Jun.

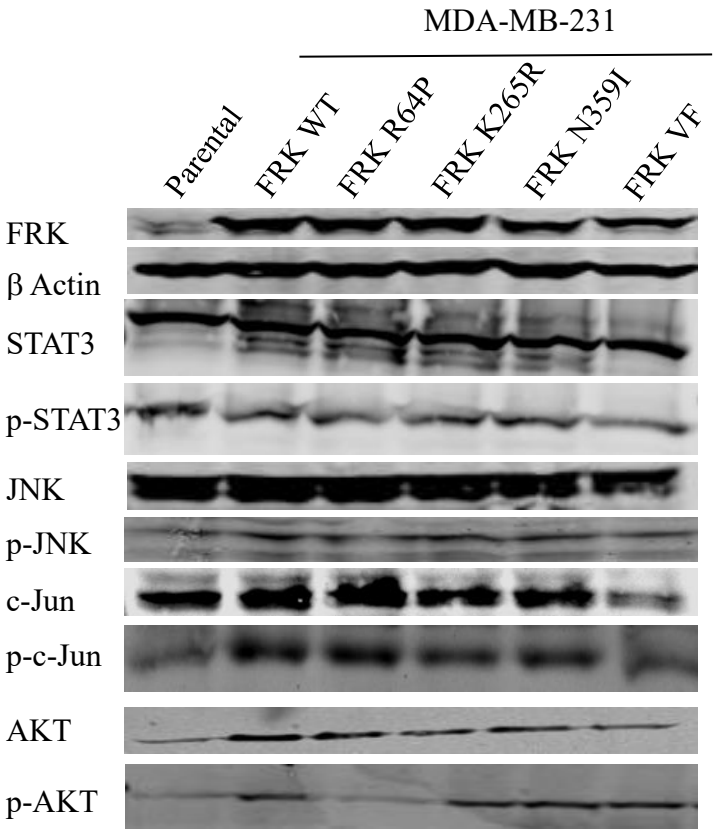

Figure 5.7.1

Effect of FRK cancer associated mutations on critical signaling molecules. Samples analyzed were, MDA-MB-231 parental, FRK WT, FRK R64P, FRK K265R, FRK N359I, and FRK VF. Antibodies for STAT3, pSTAT3 Y705, JNK, pJNK Y185, c-Jun, p-c-Jun S63, AKT, and pAKT S473.

5.7.2 FRK Mutation effect on Signaling in HEK293 Transient expression:

Since there was no effect seen in the MDA-MB-231 stable cell lines, experiments were performed on transient expression lysates in the less mutagenic cell line HEK293. This experiment produced various changes in signaling pattern. First there was no change in expression level of STAT3

however there was great variation in the phosphorylation at the tyrosine 705 site except in the N359I mutation. Next while it had been previously revealed that FRK expression is capable of reducing pJNK and p-c-Jun levels, no statistically relevant data was found from the transient expression of FRK WT and mutations. There was also no change seen in AKT, p-AKT, JNK, and p-JNK levels (**Figure 5.7.2)**.

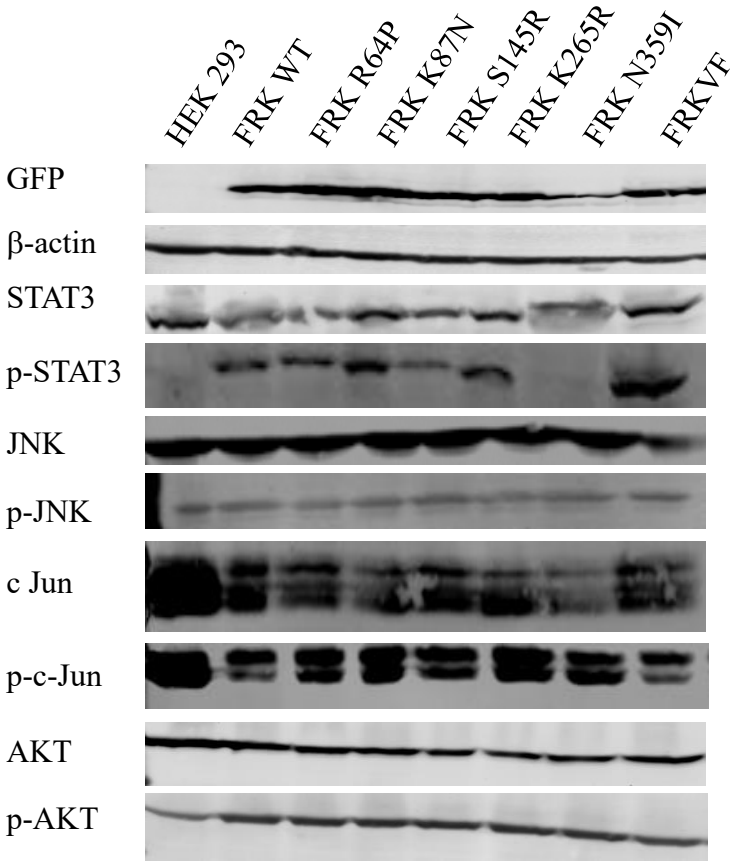

Figure 5.7.2.1

Effect of FRK cancer associated mutations on critical signaling molecules. Samples analyzed were, HEK293 parental, FRK WT, FRK R64P, FRK K87N, FRK S145R, FRK K265R, FRK N359I, and FRK VF. Antibodies for STAT3, pSTAT3 Y705, JNK, pJNK Y185, c-Jun, p-c-Jun S63, AKT, and pAKT S473.

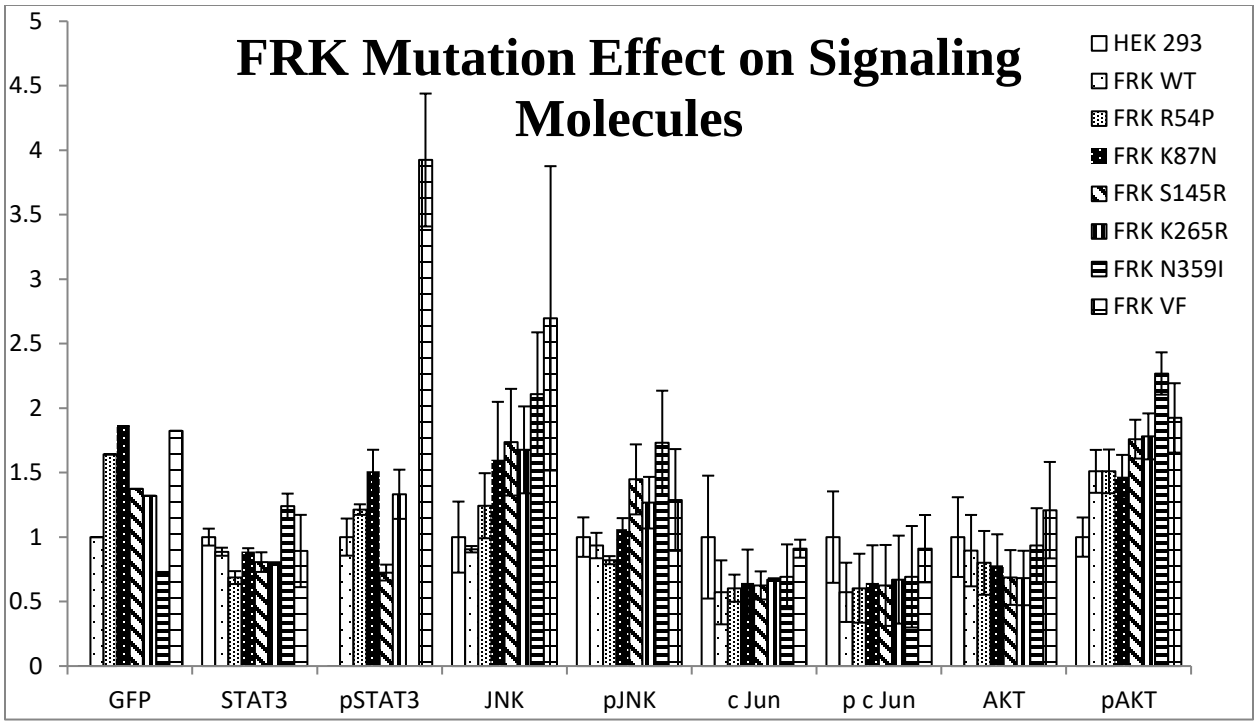

Figure 5.7.2.2

Quantification of the HEK 293 cell signaling western blot in figure 5.7.2.1.

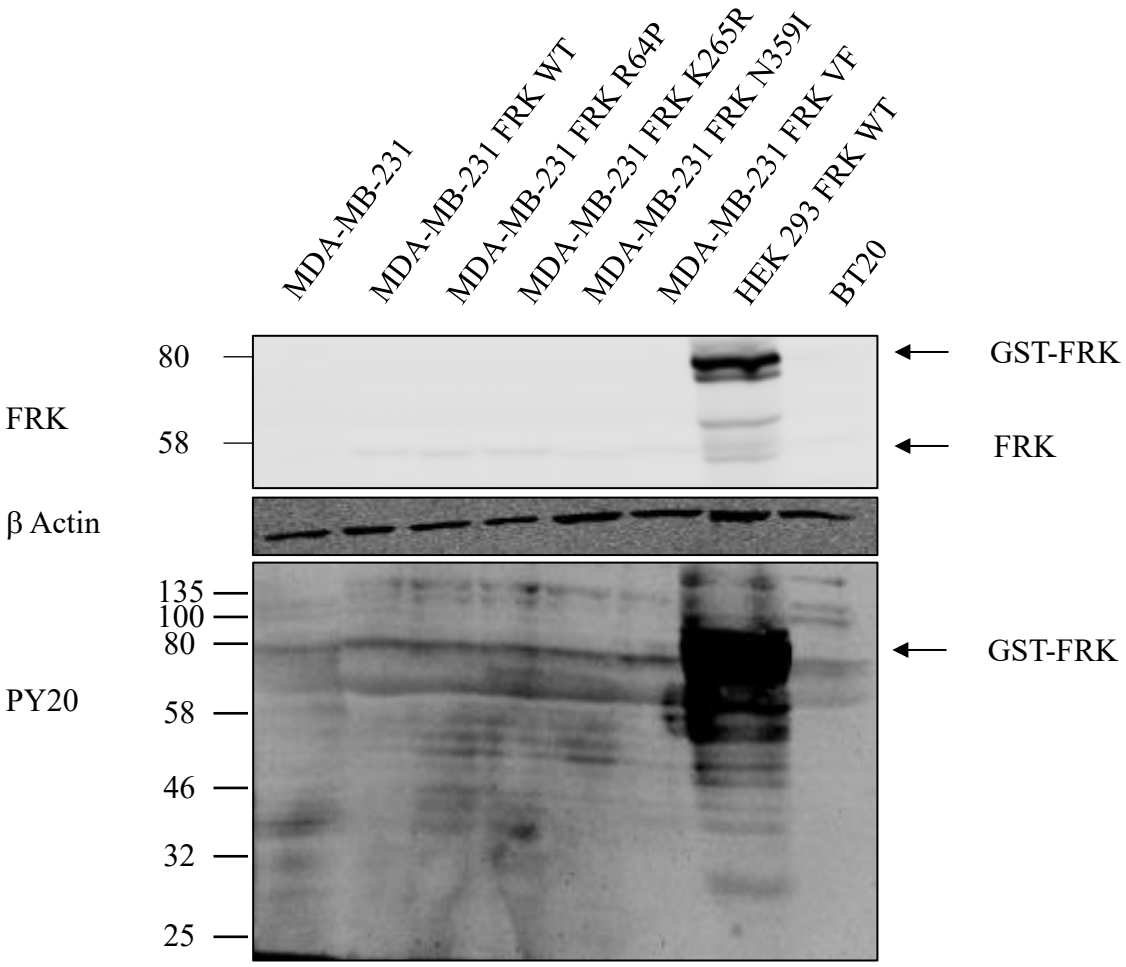

Figure 5.7.3

FRK mutation expression an activity in MDA-MB-231 stable cell lines and transiently transfected in HEK293, and parental BT20 cell line. FRK expression measured with FRK antibody, phosphotyrosine activity measured with pY20 antibody. β Actin used as loading control.

The activity of the FRK mutations stably expressed in MDA-MB-231 cells was also tested. We found that there was no activity present while FRK was expressed at detectible levels. In order to be sure that there was no issue with antibodies, two controls were utilized being WT FRK transiently expressed in HEK293 which exhibits FRK expression and activity; and BT20 lysate which has been shown to express FRK (Ogunbolude et al., 2017). The HEK293 transient transfection showed much higher expression of FRK compared to all other samples. Analyzing all MDA-MB-231 stable cell lines revealed that none of the FRK constructs expressed in MDA-MB-

231 cells possess any activity. The control FRK transiently expressed exhibited the expected activity where the BT20 showed no activity (Figure 5.7.3).

5.8 Rotational Anisotropy

These experiments involve designing peptides that are likely to interact with the protein interaction domains of FRK and linking a fluorescent marker to them, in this case fluorocein. The fluorescent marker is excited with vertically polarized light and the speed of rotation is measured with the QuantaMaster QM-4 spectrofluorometer (Photon Technology International). The smaller molecule such as the peptide alone should have the fastest rotation where the peptide bound to its interaction domain will have a much slower rotation (Jameson and Ross, 2010). With the fluorescent maker attached, the light emitted by the smaller peptide will be distributed in all directions. The larger peptide-protein complex will emit light in line with the original excitations direction in this case, vertically polarized light and result in an increase in polarization compared to the freely rotating peptide. Anisotropy is another term for the emission of polarized light, and in this case has a range from +1 to -0.5 (Jameson and Ross, 2010). The anisotropy values calculated from the experiments performed were then normalized with the highest anisotropy value labeled as 100% of the peptide bound and the freely rotating peptide labeled as 0% bound.

SH3 binding peptides were designed based on previous studies assessing interactions between GST-FRK, and PTEN, and BRCA1. These experiments identified the FRK domain responsible for interaction and the region where binding occurred on the respective protein. PXXP motifs were selected and peptides were designed with five amino acids on either side of the motif. SH2 peptides were selected from the consensus peptide determined by Zhao et al. (Zhao et al., 2013) and from the FRK C terminus.

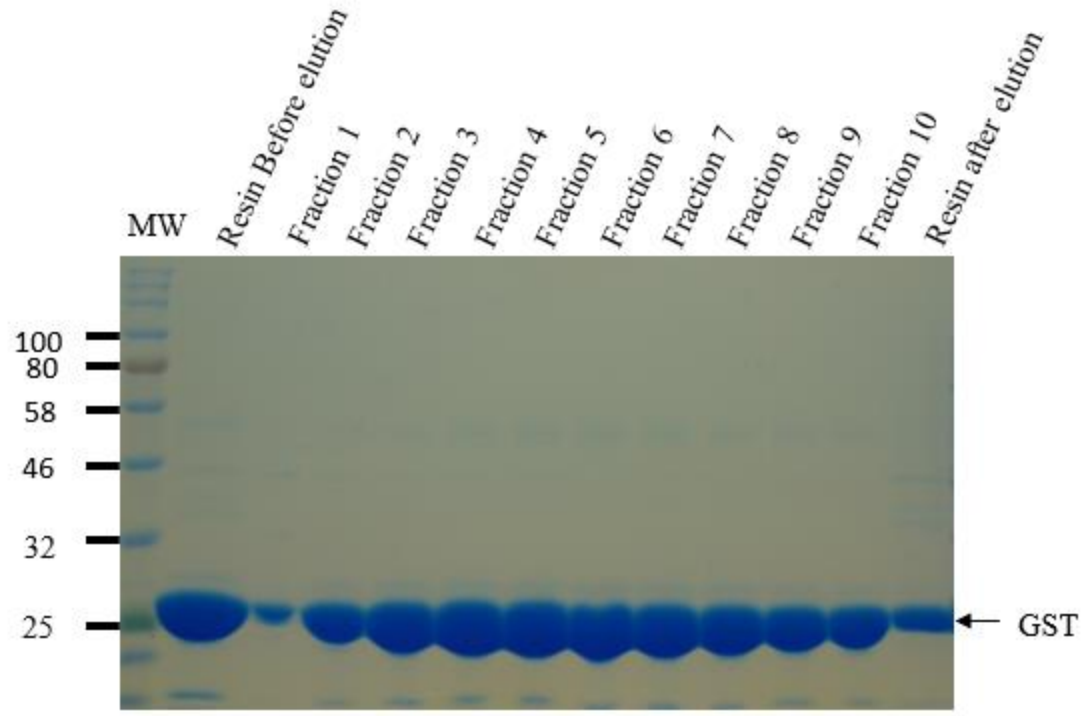

Figure 5.8.1

GST expression. Lysate from E. coli expressing GST alone for purposes of control. 10, 1 mL fractions run as well as the protein remaining on the column after elution. Protein levels shown through Coomassie staining and indicated by arrow.

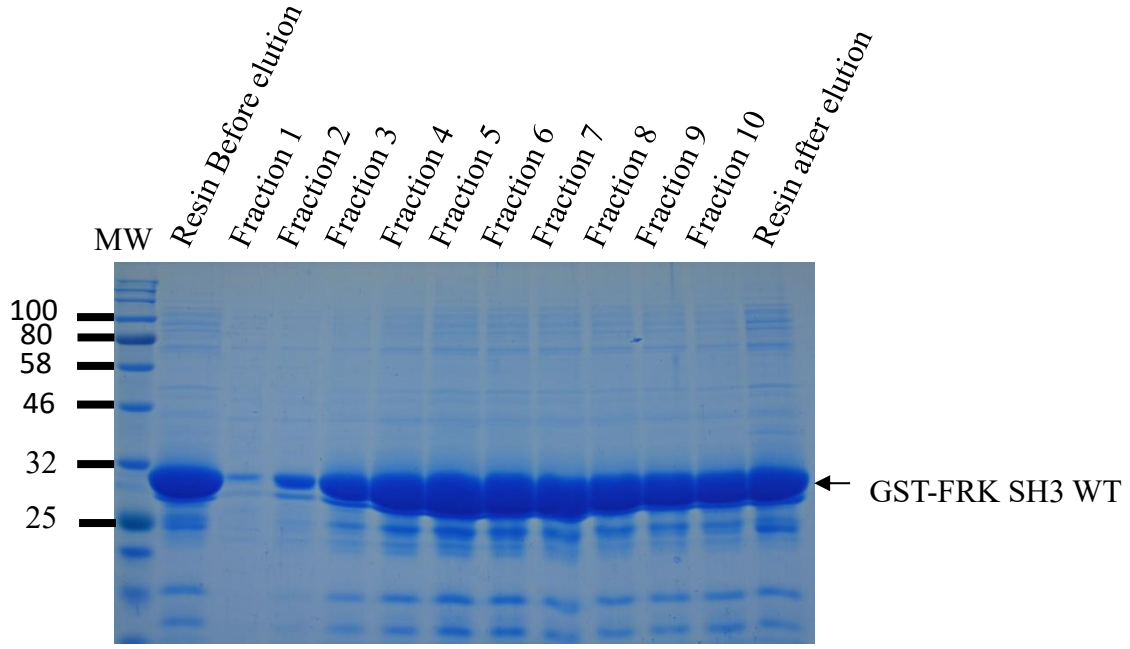

Figure 5.8.2

FRK wild type SH3 domain expression. Lysate from E. coli expressing GST-FRK SH3 WT. 10, 1 mL fractions run as well as the protein remaining on the column after elution. Protein levels shown through Coomassie staining and indicated by arrow.

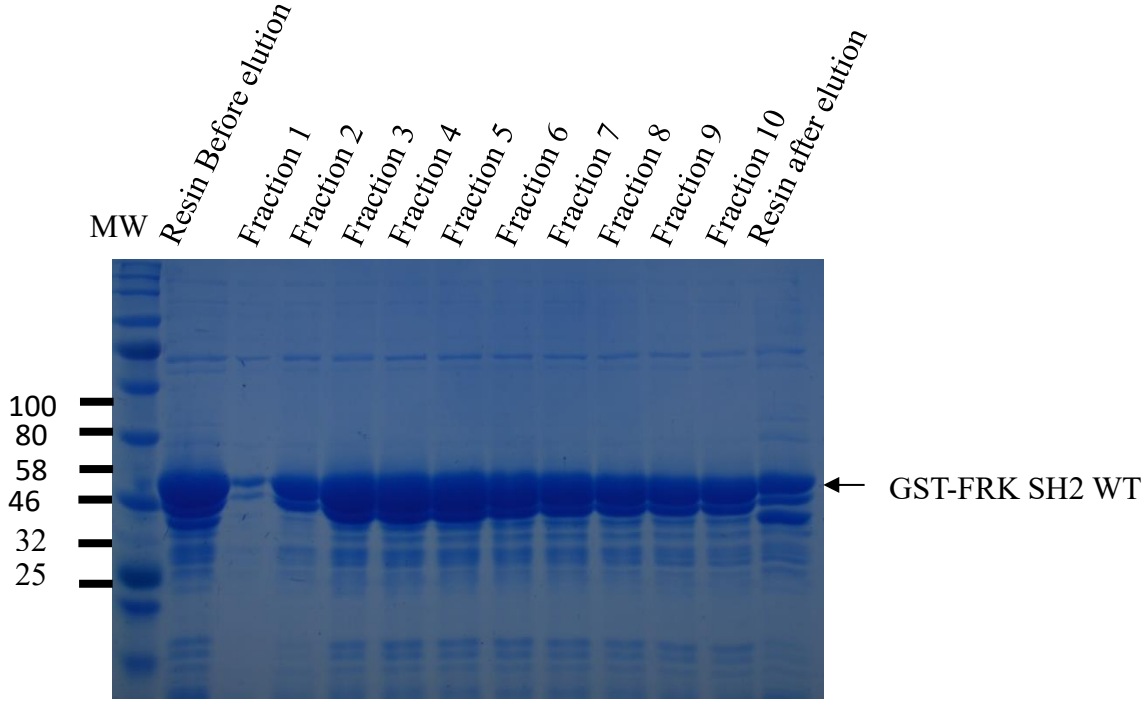

Figure 5.8.3

FRK wild type SH2 domain expression. Lysate from E. coli expressing GST-FRK SH2 WT. 10, 1 mL fractions run as well as the protein remaining on the column after elution. Protein levels shown through Coomassie staining and indicated by arrow.

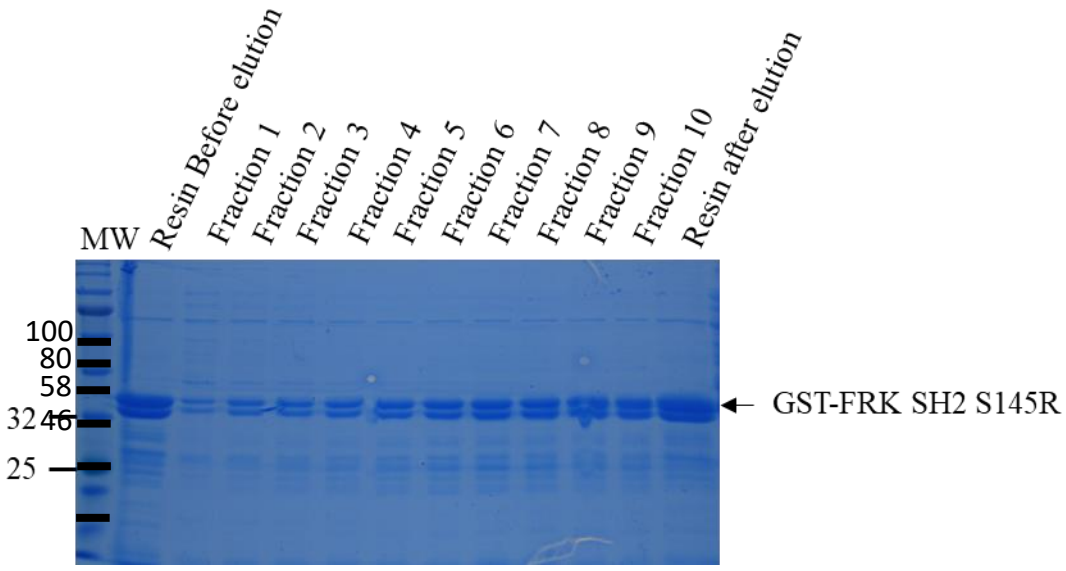

Figure 5.8.4

FRK S145R SH2 domain expression. Lysate from E. coli expressing GST-FRK SH2 S145R. 10, 1 mL fractions run as well as the protein remaining on the column after elution. Protein levels shown through Coomassie staining and indicated by arrow.

Peptide Sequence	Interaction Protein	Interaction Domain
PNVEEPSNPEASSS	PTEN	SH3
DTYLIPQIPHSHY	BRCA1	SH3
ETDSS($_p$Y)SDANN	FRK C terminus	SH2
HF(pY)ENI	Consensus Peptide	SH2

Table 5.8 1

Peptides used for rotational anisotropy. All peptides labelled with fluorocein tag. $_p$Y indicates site of phosphorylation.

5.8.1 FRK SH3 Domain Interactions:

The FRK WT SH3 domain was tested with the peptides at a concentration of 50 nM and the SH3 domain at a concentration 80 μM. Unfortunately, the FRK WT SH3 domain showed no association with PTEN and BRCA1 peptides as there was no increase in anisotropy detected (**Figures 5.81.1 and 5.8.1.2**).

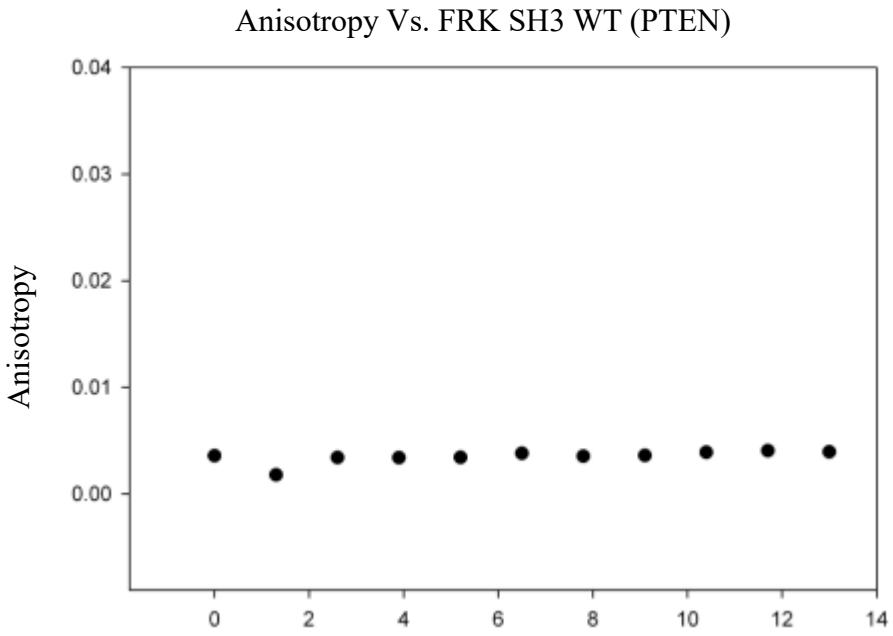

Figure 5.8.1 1

Anisotropy data for interaction with the PTEN peptide PNVEEPSNPEASSS showing no increase in anisotropy indicating no binding is occurring.

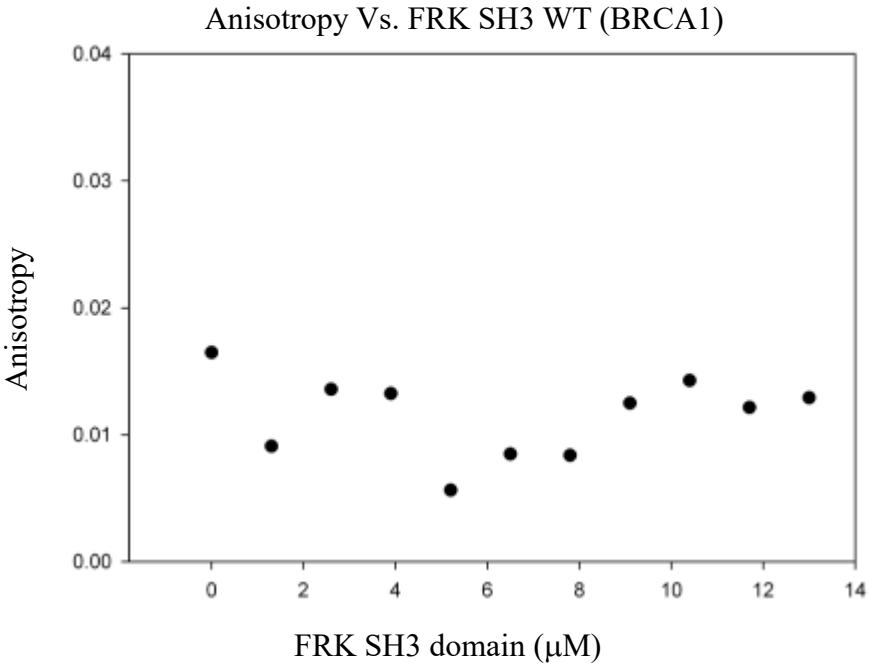

Figure 5.8.1 2

Anisotropy data for interaction with the BRCA1 peptide DTYLIPQIPHSHY showing no increase in anisotropy indicating no binding is occurring.

5.8.2 FRK SH2 WT Interactions:

5.8.2.1 FRK WT SH2 Interaction with C Terminus:

FRK WT SH2 shows a specific binding with its own C terminus as exhibited by rotational anisotropy where the FRK WT SH2 was titrated into the reaction and the anisotropy values had increased until they plateaued indicating that all of the peptide (FRK C terminus, ETDSS($_p$Y)SDANN) had been bound (Figure 5.8.2.1.1). From this the K_d value was interpreted to be 2.5 μM as was calculated by fitting a sigmoidal curve by regression analysis. This data indicates that the FRK WT SH2 domain and FRK C terminus can interact with high affinity (**Figure 5.8.2.1.1**).

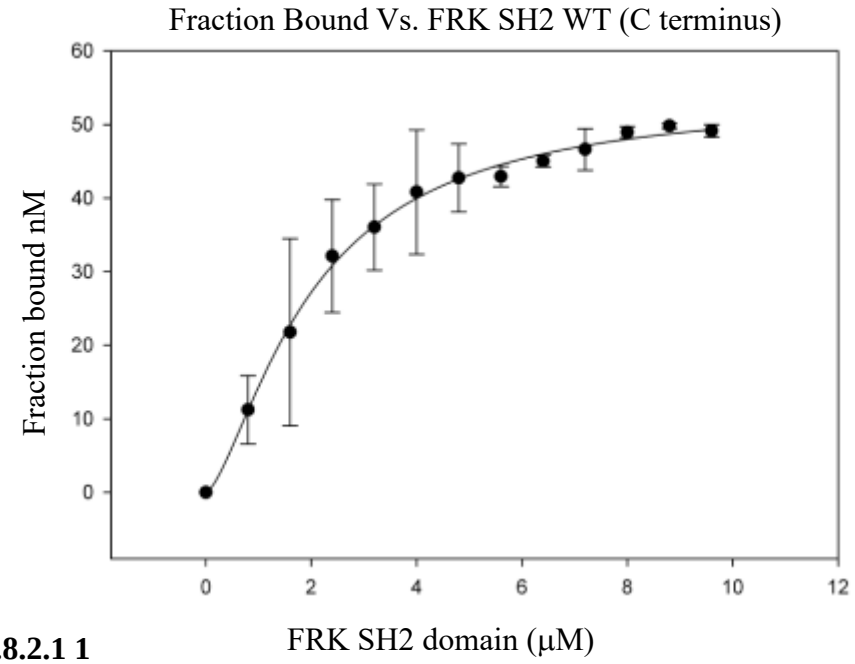

Figure 5.8.2.1 1

Rotational anisotropy was used to measure the interaction between FRK WT SH2 and FRK C terminus. Anisotrpoy data was normalized to fraction of FRK C terminus bound and a K_d value was found by regression analysis by fitting a sigmoidal curve to the average of three different experiments. K_d vaule = 2.5 μM.

5.8.2.2 FRK WT SH2 Interaction with Consensus Peptide

FRK WT SH2 shows a specific binding with the SH2 consensus peptide as exhibited by rotational anisotropy where the FRK WT SH2 was titrated into the reaction and the anisotropy values had

increased until they plateaued indicating that all of the peptide (FRK C terminus, ETDSS($_p$Y)SDANN) had been bound (Figure 5.8.2.2.1). From this the K_d value was interpreted to be 0.4 μM as was calculated by fitting a sigmoidal curve by regression analysis. This data indicates that the FRK WT SH2 domain and SH2 consensus peptide can interact with high affinity (**Figure 5.8.2.2.1)**.

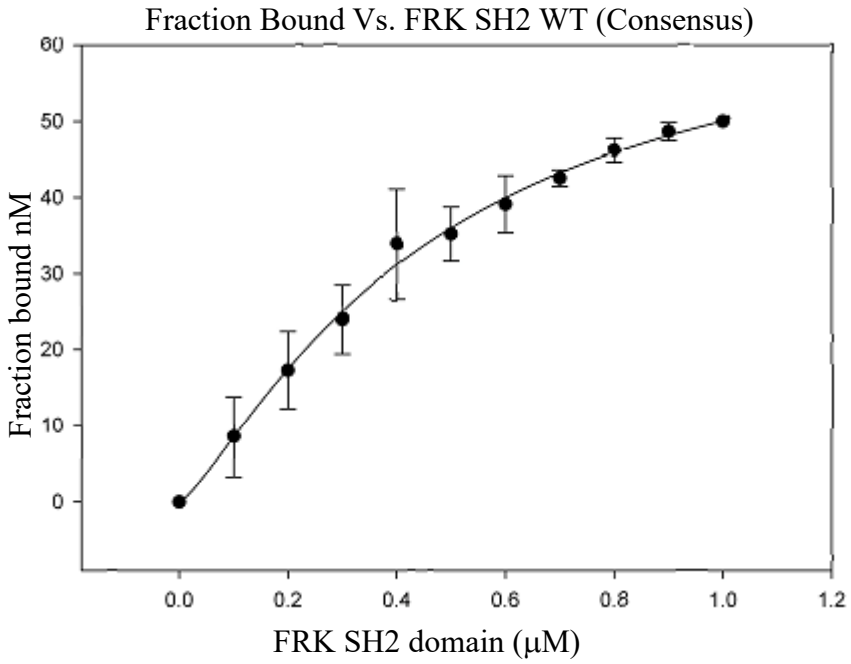

Figure 5.8.2.2 1

Rotational anisotropy was used to measure the interaction between FRK WT SH2 and consensus peptide. Anisotrpoy data was normalized to fraction of consensus peptide bound and a K_d value was found by regression analysis by fitting a sigmoidal curve to the average of three different experiments. K_d value = 0.4 μM.

5.8.3 Anisotropy Data for Interaction of GST and SH2 binding Peptides

The FRK constructs utilized were GST fusion proteins therefore, experiments were also performed with the GST protein alone in 80 μM concentrations to confirm that the interactions are specific to the SH2 domain of FRK and not GST. According to the results no binding was seen between GST and any of the SH2 domain specific peptides (**Figure 5.8.3.1, 5.8.3.2)**.

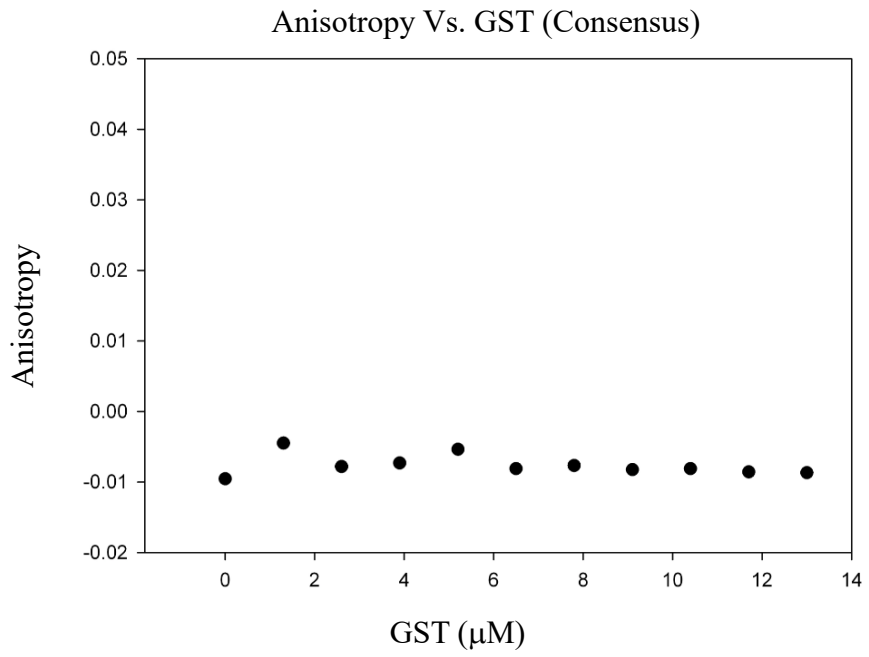

Figure 5.8.3 1

Anisotropy data for interaction with the FRK SH2 domain consensus peptide indicating no binding is occurring.

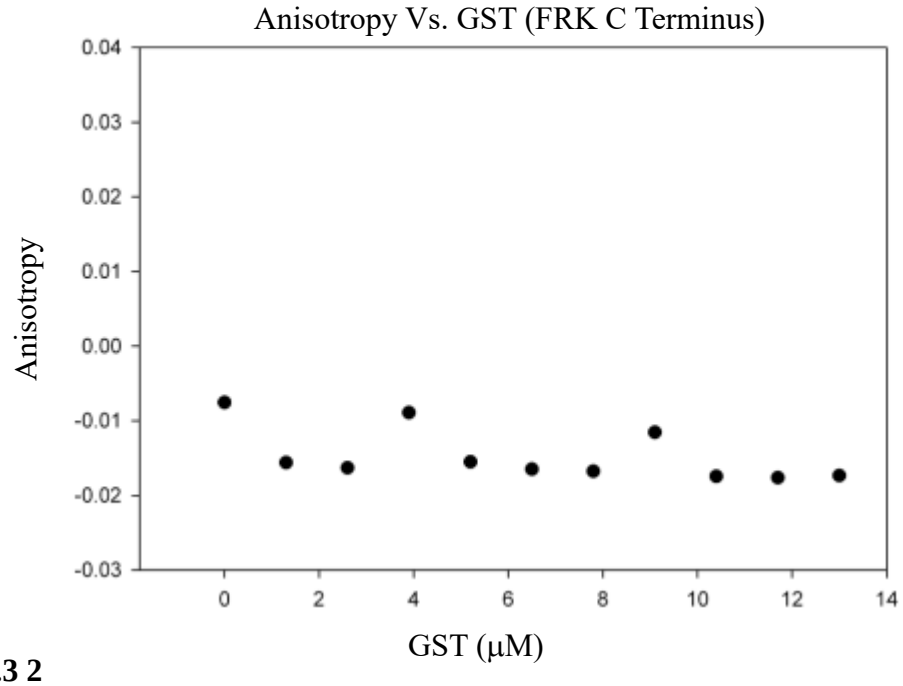

Figure 5.8.3 2

Anisotropy data for interaction with the FRK C terminus peptide indicating no binding is occurring.

5.8.4 FRK S145R SH2 Domain Interactions

5.8.4.1 FRK S145R SH2 Domain Interaction with FRK C Terminus

The mutations that are found in the SH3 and SH2 domains have the potential to disrupt inter and intramolecular interactions. We hypothesized that theses mutations would disrupt these interactions. This was tested using rotational anisotropy with the help of Dr. Linda Chelico.

FRK S145R SH2 shows a specific binding with its own C terminus as exhibited by rotational anisotropy where the FRK S145R SH2 was titrated into the reaction and the anisotropy values had increased until they plateaued indicating that all of the peptide (FRK C terminus, ETDSS($_p$Y)SDANN) had been bound (**Figure 5.8.4.1**). From this the K_d value was interpreted to be 1.4 μM as was calculated by fitting a sigmoidal curve by regression analysis. This data indicates that the FRK WT SH2 domain and FRK C terminus can interact with high affinity.

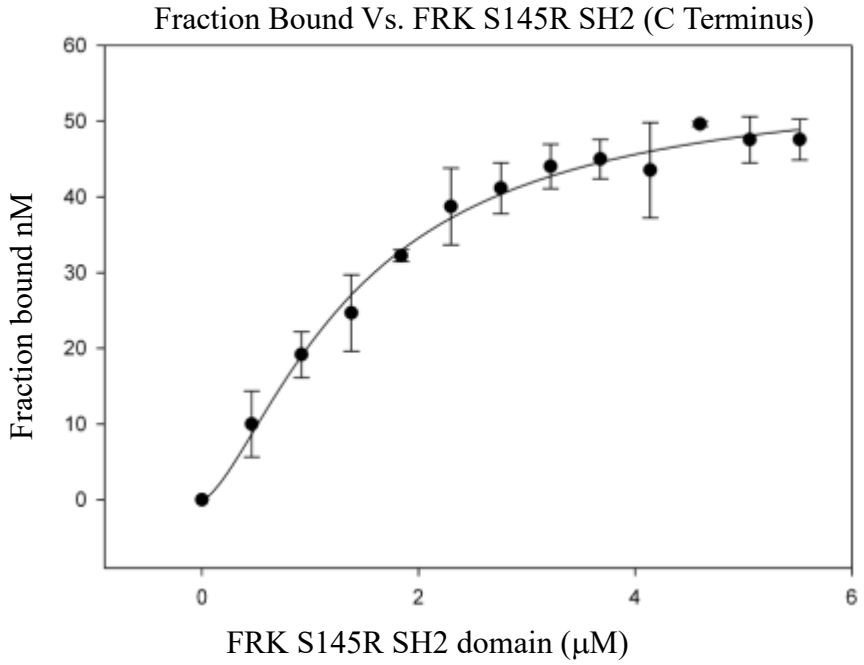

Figure 5.8.4.1

Rotational anisotropy was used to measure the interaction between FRK S145R SH2 and FRK C terminus. Anisotropy data was normalized to fraction of FRK C terminus bound and a K_d value was found by regression analysis by fitting a sigmoidal curve to the average of three different experiments. K_d value = 1.4 μM.

5.8.4.2 FRK S145R SH2 Domain Interaction with Consensus Peptide

FRK S145R SH2 shows a specific binding with its own C terminus as exhibited by rotational anisotropy where the FRK S145R SH2 was titrated into the reaction and the anisotropy values had increased until they plateaued indicating that all of the peptide (FRK consensus, HF(pY)ENI) had been bound (**Figure 5.8.4.2**). From this the K_d value was interpreted to be 0.8 μM as was calculated by fitting a sigmoidal curve by regression analysis. This data indicates that the FRK WT SH2 domain and FRK C terminus can interact with high affinity.

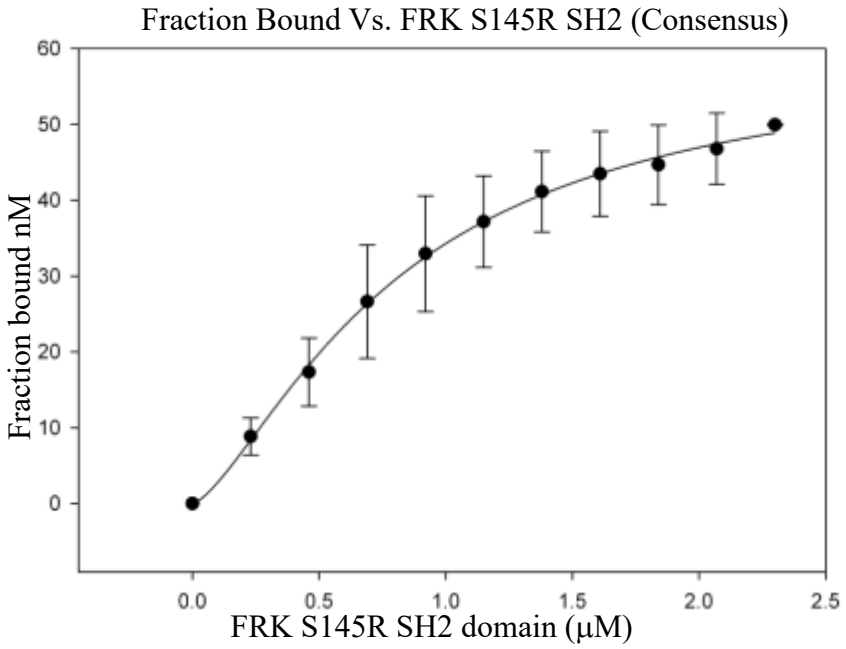

Figure 5.8.4.2

Rotational anisotropy was used to measure the interaction between FRK S145R SH2 and SH2 consensus peptide. Anisotrpoy data was normalized to fraction of SH2 consensus peptide bound and a K_d value was found by regression analysis by fitting a sigmoidal curve to the average of three different experiments. K_d vaule = 0.8 μM.

All K_d and standard error values are found in table 5.8.3.1.

Table 5.8.3.1

All K_d and standard error values from rotational anisotropy experiments.

Interaction: FRK SH2	K_d (μM)	Error
WT SH2 and FRK C terminus	2.5	0.30
WT SH2 and Consensus Peptide	0.4	0.08
S145R SH2 and FRK C terminus	1.4	0.15
S145R SH2 and Consensus peptide	0.8	0.06

6.0 Discussion:

FRK is a non-receptor tyrosine kinase which is associated with the BFK family and has been seen to function as a tumor suppressor in breast cancer and glioma (Goel and Lukong, 2016). Cancer associated mutations found in BRK have been previously characterized but those which lie in FRK have not been investigated. Six FRK cancer associated mutations have been characterized in this study in terms of their effect on proliferation, migration, invasion, and signaling. What was found was that the phospho-STAT3 was elevated in the presence of the VF deletions mutant which possesses the highest kinase activity.

6.1 Enzymatic Activity of BRK and FRK Mutations

In the present study, cancer related mutations of BRK (Tsui and Miller, 2015) were compared to mutations of similar residues in FRK (**Table 2)**. The effect of cancer related mutations in BRK were assessed via western blot utilizing a phospho-tyrosine antibody in Figure 5.2 and were compared to the mutation of those similar residues in FRK (**Figure 5.1**). Through the comparison of the tyrosine kinase activation, we observed that the mutations of these similar residues have differing effects between FRK and BRK. Only two mutations of the conserved FRK residues altered the kinase activity of FRK. The mutations which exhibited similar effects in both proteins were the V253M (BRK), V295M (FRK), N317S (BRK), and N359I (FRK). V253M and N317S completely abolished kinase activity in BRK, whereas V295M reduced activity and N359I

inactivated FRK. The N317 (BRK) and N359 (FRK) completely inactivate kinase activity of both proteins because this asparagine lies in a critical motif which is required for enzyme activity (Welsh et al., 2004). The biological importance of V253 (BRK) and V295 (FRK) is not currently known.

6.2 Cancer-Associated FRK Mutation Enzymatic Activity

6.2 FRK Cancer-Associated Mutation Activity in HEK293 Cells

The six-cancer related FRK mutations studied were, R64P, K87N, S145R, K265R, N359I, and V(378)F(379)del (**Figure 5.2.1 and 5.2.2**). Mutations in the SH3 domain and the SH2 domain (R64P, K87N, S145R) all exhibited no effect on kinase activity. The lone mutation in the SH2 domain S145R was found in a suspected phospho-tyrosine binding motif FLIRES. This mutation is thought to interrupt the interaction between target phospho-tyrosines and the FRK SH2 domain and was expected to increase kinase activity due to the loss of regulation through Y497. Previous studies performed on Abl kinase, reveal that mutations in this motif cause the reduced ability of the SH2 domain to interact with target phospho-tyrosines (Mayer et al., 1992) .

The FRK, VF del mutation exhibited a drastic increase in kinase activity; however, the mechanism which causes this increase is not currently understood. This deletion lies down stream of a conserved motif DFG which aids in the binding of ATP. This deletion may disrupt how ATP interacts with the kinase domain resulting in increased activity.

Two mutations showed reduced kinase activity, those being K265R, and N359I. The ATP binding lysine in FRK is K262, so it is possible that K265 may play a lesser role in ATP binding and could explain the reduction in kinase activity. The N359I mutation abolishes kinase activity due to its placement in the motif critical for enzyme activity. This mutation lies in a highly conserved region among the BFK family. This asparagine may interact directly with ATP and with a critical motif “HRD”. The aspartate residue has been shown to be the catalytic residue aiding the breakdown of ATP. Mutating the asparagine to isoleucine disrupts the interaction between both ATP and the aspartate of the HRD motif which results in abolished kinase activity.

6.3 Effect of Cancer-Associated Mutations on Cell Proliferation and Cell Migration

We next investigated the effect of each of these mutations on the rate of cell growth (**Figure 5.4.2**). We initially predicted that the mutants with elevated kinase activity would possess an increased anti-proliferative activity. Transducing wild type FRK into MDA-MB-231 cells resulted in a decreased rate of cell proliferation which is consistent with what has been seen in previous studies (Ogunbolude et al., 2017b). The mutation studied which exhibited elevated kinase activity was the VF deletion which was expected to enhance the anti-proliferative effects of FRK. The mutations which result in decreased kinase activity were K265R, N359I were expected to diminish the function of FRK. All mutations resulted in reduced cell proliferation compared to the MDA-MB-231 cell line but the rates if proliferation were not statistically different from the wild type FRK. Migration was then analyzed using a wound healing assay (**Figure 5.5.1**). The wild type FRK resulted in a significant decrease in the rate of wound closure which is significant with past findings (p value < 0.001) (Ogunbolude et al., 2017b). Mutations R64P, K265R, and N359I all behaved in a similar manner which exhibited an increased migration rate compared to wild type FRK and resulted in a wound 38-42% open which is significant compared to the wild type FRK and VF mutation (p value < 0.05). The VF Mutation showed a slower rate of migration compared to the other mutations but even with its heightened activity it was not statistically different from the wild type FRK. These results surrounding the effects on cell proliferation and migration indicate that the effects that FRK exerts on these cellular processes are not kinase dependent.

6.4 Effect of Mutations on Cell Invasion

The invasion was assessed using a Boyden chamber coated in extracellular matrix and polycarbonate membrane with an 8.0 μm pore size. The cells used were the MDA-MB-231, and MDA-MB-231 cell lines stably expressing FRK WT, FRK R64P, FRK K265R, and FRK VF (**Figure 5.6.1**). The MDA-MB-231 control produced the highest number of migratory cells and the FRK WT stable cell line had the fewest migratory cells (p value < 0.05) which is consistent with what our lab has found previously (Ogunbolude et al., 2017). We hypothesized that the activity of each mutation would directly affect the rates of invasion with the higher activity mutations (R64P, VF) providing anti-invasive properties where the lower activity mutations (K265R, N359I) reduce the anti-invasive effects of FRK in breast cancer. FRK WT was the only test which showed a reduction in cell invasion while all mutations tested all resulted in a similar

number of cells which were able to migrate through the membrane as the MDA-MB-231 control. This indicates that the level of kinase activity of FRK is not the only factor that affects the invasive potential of these stable cell lines.

6.5 Effect of FRK Mutations of Cell Signaling Molecules

6.5.1 Effect Seen in MDA-MB-231 Stable Cell Lines

The signaling molecules analyzed were STAT3, and p-STAT3 (Y705), JNK, p-JNK (Y185), c-Jun, p-c-Jun (S63), and AKT, p-AKT (S473) which have all been seen to be altered due to FRK expression in breast cancer and glioblastoma (Ogunbolude et al., 2017; Zhou et al., 2012). Increased activation in any of these signalling molecules would increase cell proliferation and invasive potential of these cell lines. There was no change seen in the selected signalling molecules within the stable cell lines. This could be due the level of mutagenicity associated with the MDA-MB-231 cell line or the lack of FRK kinase activity as shown previously which suggests that FRK alters these signaling pathways in a kinase dependent manner. If FRK expression had remained it would be expected that the STAT3 phosphorylation would have been reduced in a kinase dependant manner as shown in Ogunbolude et al., 2017, which would have also reduced the growth capabilities of the stable cell line. Perhaps a transient transfection into MDA-MB-231 cells would produce FRK with kinase activity and result in a possible effect on these signaling molecules.

6.5.2 Effect Seen in Transiently Transfected HEK293 Cells

The same signaling molecules were tested for by transiently transfecting HEK 293 cells which produced differing results compared to the MDA-MB-231 stable cell lines (**Figure 5.7.2.1**). The main effect occurred in the STAT3 and p-STAT3 trials. There was no p-STAT3 detected in the HEK293 cell line where WT FRK and all mutations except for N359I producing higher levels of p-STAT3. The kinase dead mutant was unable to induce STAT3 phosphorylation where all other mutants were able. This observation suggests that FRK is capable of increasing p-STAT3 levels in a kinase dependent manner. This was highlighted by the increased p-STAT3 induction by the VF mutant which produced significantly higher levels of p-STAT than all other mutations. No other statistically significant event was detected in any of the other signaling molecule tests including JNK, c-Jun, and AKT. The significance of the induction of STAT3 phosphorylation is that STAT3 is responsible for the transcription of genes required for growth and cell survival. In

the context of HEK293 cells, the introduction of FRK may increase the growth rate of these cells through the activation of STAT3.

6.6 FRK Cancer-Associated Mutation Activity in MDA-MB-231 Cells

The kinase activity of these FRK cancer-associated mutations was also assessed in the MDA-MB-231 stable cell lines. Surprisingly, none of the mutations nor the WT FRK in MDA-MB-231 cells showed any activity, where the control FRK WT transiently expressed in HEK293 cells showed proved to be active. This could possibly be because the MDA-MB-231 cells express higher levels of a phosphatase that dephosphorylates the Y387 in FRK which is the autophosphorylation site. This could also be due to the use of polyclonal experimentation. As the cells were passaged, the level of FRK activity and expression slowly decreased . The cell population may have been overrun by the fastest growing clone which expressed FRK in the level shown in figure 5.7.3. This decreased FRK expression could explain the results seen in the invasion assay.

6.7 Rotational Anisotropy

Rotational anisotropy was used to analyze the binding of each FRK domain to a peptide sequence which was thought to interact with each domain. Two peptides were used for each domain where the SH3 peptide was paired with either a peptide possessing PXXP from BRCA1 or PTEN. The SH2 domain was paired with peptide sequences possessing a phosphorylated tyrosine near the center of the peptide. These peptides were from the C terminus of FRK and what had been experimentally determined to be the consensus FRK SH2 binding sequence.

6.7.1 FRK WT SH3 Domain Interactions

The FRK SH3 domain was tested for binding to peptides derived from PTEN and BRCA1 at increasing peptide concentrations of 1.3 μM at each titration. Unfortunately, neither of the peptides was capable of binding to the FRK SH3 domain. The SH3 domain may interact with its target in a different manner than originally thought. In these cases, the target may need to be folded to provide the correct binding sequence.

6.7.2 FRK WT SH2 Domain Interactions

The FRK SH2 domain was used at differing concentrations for each peptide. For the SH2 consensus peptide, FRK WT SH2 was added at 0.6 μM at each titration and for the FRK C

terminus, FRK WT SH2 was added at 0.1 μM at each titration. Interactions were seen for each peptide. The K_d associated for the interaction with the SH2 consensus peptide was 0.4 μM and the K_d for the FRK C terminus interaction was 2.5 μM. Identical experiments were performed for GST alone as the FRK constructs were fused to GST. No binding was observed for the GST alone experiments.

6.7.3 FRK S145R SH2 Domain Interactions

S145R mutant was added at concentrations of 0.2 μM at each titration and interacted with both peptides. The K_d for the consensus peptide was 0.8 μM and the K_d for the FRK C terminus was 1.4 μM. These numbers are slightly different from the K_ds for the FRK WT SH2 domain but there is not a large enough of a change to say they are behaving differently. It was surprising to see the S145R mutant binding to the SH2 peptides, however, this indicates that S145 is not the only important residue involved in phosphotyrosine binding. These results indicate that the S145R mutation in FRK does not have the same effect on phosphotyrosine binding as this analogous mutation in Abl kinase had. Amino acids in the FLIRES motif may have differential roles in the binding of phosphotyrosines in different kinases.

7.0 Conclusions:

A series of FRK cancer-associated mutations were generated where their kinase activity, effect on cell proliferation, migration, invasion, signaling molecules, and interactions with SH3 and SH2 binding peptides were all assessed. The activities of the mutations transiently expressed in HEK293 showed significant variation for a number of mutations although, three of the mutations showed no change compared to the wild type FRK. The three mutations which showed no change in kinase activity were R64P, K87N, and S145R. Two mutations exhibited a reduction of kinase activity those being K265R, and N359I with the latter showing no kinase activity. The last remaining mutation is the VF deletion in the kinase domain, which show 3.5-fold increase in kinase activity.

Four mutations were chosen to be expressed stably in MDA-MB-231 cells and activity was also tested for. Unfortunately, none of the mutations exhibited any kinase activity when assessed through Western blot. Still the stable cell lines were used to test cell proliferation, migration and

invasion. All cancer associated mutations resulted in decreased cell proliferation but were no different from each other. Wild type FRK had the most drastic reduction in cell migration that was equal to that of VF. R64P, K265R, and N359I all showed slightly less effectiveness in reducing cell migration. The invasion assay shows that only the wild type FRK was capable of reducing the invasiveness of MDA-MB-231 cells.

The effect of these mutations were also tested as to how they can alter the phosphorylated levels of STAT3, c-Jun, JNK, and AKT. The stable MDA-MB-231 cell lines showed no change in phosphorylation levels of these proteins. The same experiments were performed on HEK293 cells transiently expressing all mutations. Only p-STAT3 Y705 levels were altered where all FRK constructs showed increased p-STAT3 levels with VF showing the largest increase with the exception of N359I which had no effect on STAT3 phosphorylation. This indicated that this event occurs in a kinase dependent manner.

Interaction experiments were conducted utilizing the three mutations found in the SH3 and SH2 domains. The SH3 peptides designed were identified from known interaction partners PTEN and BRCA1 and the SH2 peptides were from the C terminus of FRK and the consensus SH2 peptide determined by Zhao et al. (Zhao et al., 2013). The SH3 domain unfortunately did not show any interaction with the peptides associated with PTEN or BRCA1. The wild type FRK SH2 domain did interact with both the C terminus of FRK and the consensus SH2 peptide with a K_d of 2.5 μM and 0.4 μM respectively. The S145R SH2 mutation also associated with both the C terminus and consensus peptides with a K_d of 1.4 μM and 0.8 μM. These numbers are close enough to state that these domains are behaving in a similar manner, which means that the S145R mutation does not have a significant effect of phosphotyrosine binding.

8.0 Future Directions

Considering how the mutations chosen to be stably expressed in MDA-MB-231 cells showed no activity, they should be expressed in either a less mutagenic breast cancer such as cell line such as MCF7 or using a Tet on system. In order to express the FRK mutants in MCF7 first they wild type FRK would have to be knocked out so that the only FRK effect seen will be from the specific mutations. Stable cell lines should also be generated in the HEP3B liver cancer cell line to determine if the effects produced by the FRK mutations are exclusive to the tissue type or are

solely based on the kinase activity. The Tet on system may be important for expressing the FRK mutants in MDA-MB-231 cells as it may be a possibility that the stable overexpression of FRK would result in additional changes occurring within the cell that cause FRK activity to be shut down.

The binding experiments resulted in equal binding between the wild type FRK SH2 domain and the S145R SH2 mutation. This mutation was hypothesized to disrupt the interaction between FRK and may indicate that phosphorylated tyrosine residues. This the different residues found within the FLIRES motif may play different roles in the binding of phosphotyrosines in different kinases. To discover which residues are of the utmost importance, each residue should be mutated individually, and the same rotational anisotropy experiments redone to observe changes in binding. To also be absolutely certain that this motif is required for phosphotyrosine binding, the entire motif should be removed to observe that no peptide binds. The SH3 peptides also showed no interaction with the peptides associated with PTEN or BRCA1 so instead of taking peptides 15 amino acids long, the entire region where FRK binds to these proteins could be expressed by a bacterial, or SF9 expression vector and tagged with fluorescein. The rotational anisotropy experiments would then be repeated to observe binding with the entire region that FRK has been seen to associate with. Lastly, additional binding experiments should be performed using unphosphorylated peptides as a negative control.

References

Al Zaid Siddiquee, K., and Turkson, J. (2008). STAT3 as a target for inducing apoptosis in solid and hematological tumors. Cell Research *18*, 254.

An, X., Tiwari, A.K., Sun, Y., Ding, P.R., Ashby, C.R., Jr., and Chen, Z.S. (2010). BCR-ABL tyrosine kinase inhibitors in the treatment of Philadelphia chromosome positive chronic myeloid leukemia: a review. Leuk Res *34*, 1255-1268.

Avruch, J., Khokhlatchev, A., Kyriakis, J.M., Luo, Z., Tzivion, G., Vavvas, D., and Zhang, X.F. (2001). Ras activation of the Raf kinase: tyrosine kinase recruitment of the MAP kinase cascade. Recent Prog Horm Res *56*, 127-155.

Bader, A.G., Kang, S., Zhao, L., and Vogt, P.K. (2005). Oncogenic PI3K deregulates transcription and translation. Nat Rev Cancer *5*, 921-929.

Bagu, E.T., Miah, S., Dai, C., Spriggs, T., Ogunbolude, Y., Beaton, E., Sanders, M., Goel, R.K., Bonham, K., and Lukong, K.E. (2017). Repression of Fyn-related kinase in breast cancer cells is associated with promoter site-specific CpG methylation. Oncotarget *8*, 11442-11459.

Barker, K.T., Jackson, L.E., and Crompton, M.R. (1997). BRK tyrosine kinase expression in a high proportion of human breast carcinomas. Oncogene *15*, 799-805.

Berclaz, G., Altermatt, H.J., Rohrbach, V., Dreher, E., Ziemiecki, A., and Andres, A.C. (2000). Hormone-dependent nuclear localization of the tyrosine kinase iyk in the normal human breast epithelium and loss of expression during carcinogenesis. Int J Cancer *85*, 889-894.

Bibbins, K.B., Boeuf, H., and Varmus, H.E. (1993). Binding of the Src SH2 domain to phosphopeptides is determined by residues in both the SH2 domain and the phosphopeptides. Mol Cell Biol *13*, 7278-7287.

Bos, T.J., Monteclaro, F.S., Mitsunobu, F., Ball, A.R., Jr., Chang, C.H., Nishimura, T., and Vogt, P.K. (1990). Efficient transformation of chicken embryo fibroblasts by c-Jun requires structural modification in coding and noncoding sequences. Genes Dev *4*, 1677-1687.

Brauer, P.M., and Tyner, A.L. (2009). RAKing in AKT: a tumor suppressor function for the intracellular tyrosine kinase FRK. Cell Cycle *8*, 2728-2732.

Brauer, P.M., and Tyner, A.L. (2010). Building a better understanding of the intracellular tyrosine kinase PTK6 - BRK by BRK. Biochim Biophys Acta *1806*, 66-73.

Buss, J.E., Kamps, M.P., Gould, K., and Sefton, B.M. (1986). The absence of myristic acid decreases membrane binding of p60src but does not affect tyrosine protein kinase activity. J Virol *58*, 468-474.

Campbell, S.J., and Jackson, R.M. (2003). Diversity in the SH2 domain family phosphotyrosyl peptide binding site. Protein Eng *16*, 217-227.

Cance, W.G., Craven, R.J., Bergman, M., Xu, L., Alitalo, K., and Liu, E.T. (1994). Rak, a novel nuclear tyrosine kinase expressed in epithelial cells. Cell Growth Differ *5*, 1347-1355.

Cantley, L.C. (2002). The phosphoinositide 3-kinase pathway. Science *296*, 1655-1657.

Cantley, L.C., and Neel, B.G. (1999). New insights into tumor suppression: PTEN suppresses tumor formation by restraining the phosphoinositide 3-kinase/AKT pathway. Proc Natl Acad Sci U S A *96*, 4240-4245.

Cetkovic, H., Grebenjuk, V.A., Muller, W.E., and Gamulin, V. (2004). Src proteins/src genes: from sponges to mammals. Gene *342*, 251-261.

Chandrasekharan, S., Qiu, T.H., Alkharouf, N., Brantley, K., Mitchell, J.B., and Liu, E.T. (2002). Characterization of mice deficient in the Src family nonreceptor tyrosine kinase Frk/rak. Mol Cell Biol *22*, 5235-5247.

Cheng, H.C., Johnson, T.M., Mills, R.D., Chong, Y.P., Chan, K.C., and Culvenor, J.G. (2010). Allosteric networks governing regulation and catalysis of Src-family protein tyrosine kinases: implications for disease-associated kinases. Clin Exp Pharmacol Physiol *37*, 93-101.

Cooper, J.A., Gould, K.L., Cartwright, C.A., and Hunter, T. (1986). Tyr527 is phosphorylated in pp60c-src: implications for regulation. Science *231*, 1431-1434.

Cooper, J.A., and Howell, B. (1993). The when and how of Src regulation. Cell *73*, 1051-1054.

Craven, R.J., Cance, W.G., and Liu, E.T. (1995). The nuclear tyrosine kinase Rak associates with the retinoblastoma protein pRb. Cancer Res *55*, 3969-3972.

Denley, S.M., Jamieson, N.B., McCall, P., Oien, K.A., Morton, J.P., Carter, C.R., Edwards, J., and McKay, C.J. (2013). Activation of the IL-6R/Jak/stat pathway is associated with a poor outcome in resected pancreatic ductal adenocarcinoma. J Gastrointest Surg *17*, 887-898.

Feng, S., Chen, J.K., Yu, H., Simon, J.A., and Schreiber, S.L. (1994). Two binding orientations for peptides to the Src SH3 domain: development of a general model for SH3-ligand interactions. Science *266*, 1241-1247.

Giubellino, A., Burke, T.R., Jr., and Bottaro, D.P. (2008). Grb2 signaling in cell motility and cancer. Expert Opin Ther Targets *12*, 1021-1033.

Goel, R.K., and Lukong, K.E. (2015). Tracing the footprints of the breast cancer oncogene BRK - Past till present. Biochim Biophys Acta *1856*, 39-54.

Goel, R.K., and Lukong, K.E. (2016). Understanding the cellular roles of Fyn-related kinase (FRK): implications in cancer biology. Cancer Metastasis Rev *35*, 179-199.

Goel, R.K., Miah, S., Black, K., Kalra, N., Dai, C., and Lukong, K.E. (2013). The unique N-terminal region of SRMS regulates enzymatic activity and phosphorylation of its novel substrate docking protein 1. FEBS J *280*, 4539-4559.

Haegebarth, A., Bie, W., Yang, R., Crawford, S.E., Vasioukhin, V., Fuchs, E., and Tyner, A.L. (2006). Protein tyrosine kinase 6 negatively regulates growth and promotes enterocyte differentiation in the small intestine. Mol Cell Biol *26*, 4949-4957.

Hanahan, D., and Weinberg, R.A. (2011). Hallmarks of cancer: the next generation. Cell *144*, 646-674.

Hauck, C.R., Sieg, D.J., Hsia, D.A., Loftus, J.C., Gaarde, W.A., Monia, B.P., and Schlaepfer, D.D. (2001). Inhibition of focal adhesion kinase expression or activity disrupts epidermal growth factor-stimulated signaling promoting the migration of invasive human carcinoma cells. Cancer Res *61*, 7079-7090.

Hosoya, N., Qiao, Y., Hangaishi, A., Wang, L., Nannya, Y., Sanada, M., Kurokawa, M., Chiba, S., Hirai, H., and Ogawa, S. (2005). Identification of a SRC-like tyrosine kinase gene, FRK, fused with ETV6 in a patient with acute myelogenous leukemia carrying a t(6;12)(q21;p13) translocation. Genes Chromosomes Cancer *42*, 269-279.

Hu, G., Dasari, S., Asmann, Y.W., Greipp, P.T., Knudson, R.A., Benson, H.K., Li, Y., Eckloff, B.W., Jen, J., Link, B.K., *et al.* (2018). Targetable fusions of the FRK tyrosine kinase in ALK-negative anaplastic large cell lymphoma. Leukemia *32*, 565-569.

Hua, L., Zhu, M., Song, X., Wang, J., Fang, Z., Zhang, C., Shi, Q., Zhan, W., Wang, L., Meng, Q., *et al.* (2014). FRK suppresses the proliferation of human glioma cells by inhibiting cyclin D1 nuclear accumulation. J Neurooncol *119*, 49-58.

Jameson, D.M., and Ross, J.A. (2010). Fluorescence polarization/anisotropy in diagnostics and imaging. Chemical reviews *110*, 2685-2708.

Jin, L., and Craven, R.J. (2014). The Rak/Frk tyrosine kinase associates with and internalizes the epidermal growth factor receptor. Oncogene *33*, 326-335.

Jove, R., and Hanafusa, H. (1987). Cell transformation by the viral src oncogene. Annu Rev Cell Biol *3*, 31-56.

Kaplan, D.R., Whitman, M., Schaffhausen, B., Pallas, D.C., White, M., Cantley, L., and Roberts, T.M. (1987). Common elements in growth factor stimulation and oncogenic transformation: 85 kd phosphoprotein and phosphatidylinositol kinase activity. Cell *50*, 1021-1029.

Karin, M. (1995). The regulation of AP-1 activity by mitogen-activated protein kinases. J Biol Chem *270*, 16483-16486.

Keilhack, H., Tenev, T., Nyakatura, E., Godovac-Zimmermann, J., Nielsen, L., Seedorf, K., and Bohmer, F.D. (1998). Phosphotyrosine 1173 mediates binding of the protein-tyrosine phosphatase SHP-1 to the epidermal growth factor receptor and attenuation of receptor signaling. Journal of Biological Chemistry *273*, 24839-24846.

Kim, J.L., Ha, G.H., Campo, L., Denning, M.F., Patel, T.B., Osipo, C., Lin, S.Y., and Breuer, E.K. (2015). The role of Rak in the regulation of stability and function of BRCA1. Oncotarget.

Kohmura, N., Yagi, T., Tomooka, Y., Oyanagi, M., Kominami, R., Takeda, N., Chiba, J., Ikawa, Y., and Aizawa, S. (1994). A novel nonreceptor tyrosine kinase, Srm: cloning and targeted disruption. Mol Cell Biol *14*, 6915-6925.

Lee, J., Wang, Z., Luoh, S.M., Wood, W.I., and Scadden, D.T. (1994). Cloning of FRK, a novel human intracellular SRC-like tyrosine kinase-encoding gene. Gene *138*, 247-251.

Leppa, S., and Bohmann, D. (1999). Diverse functions of JNK signaling and c-Jun in stress response and apoptosis. Oncogene *18*, 6158-6162.

Li, J., Yen, C., Liaw, D., Podsypanina, K., Bose, S., Wang, S.I., Puc, J., Miliaresis, C., Rodgers, L., McCombie, R., *et al.* (1997). PTEN, a putative protein tyrosine phosphatase gene mutated in human brain, breast, and prostate cancer. Science *275*, 1943-1947.

Lim, W.A., Richards, F.M., and Fox, R.O. (1994). Structural determinants of peptide-binding orientation and of sequence specificity in SH3 domains. Nature *372*, 375-379.

Luttrell, L.M., Hawes, B.E., van Biesen, T., Luttrell, D.K., Lansing, T.J., and Lefkowitz, R.J. (1996). Role of c-Src tyrosine kinase in G protein-coupled receptor- and Gbetagamma subunit-mediated activation of mitogen-activated protein kinases. J Biol Chem *271*, 19443-19450.

Maehama, T., and Dixon, J.E. (1998). The tumor suppressor, PTEN/MMAC1, dephosphorylates the lipid second messenger, phosphatidylinositol 3,4,5-trisphosphate. J Biol Chem *273*, 13375-13378.

Manning, B.D., and Cantley, L.C. (2007). AKT/PKB signaling: navigating downstream. Cell *129*, 1261-1274.

Martin, G.S. (2001). The hunting of the Src. Nature reviews. Molecular cell biology *2*, 467-475.

Mayer, B.J., Hamaguchi, M., and Hanafusa, H. (1988). A novel viral oncogene with structural similarity to phospholipase C. Nature *332*, 272-275.

Mayer, B.J., Jackson, P.K., Van Etten, R.A., and Baltimore, D. (1992). Point mutations in the abl SH2 domain coordinately impair phosphotyrosine binding in vitro and transforming activity in vivo. Mol Cell Biol *12*, 609-618.

Menard, S., Tagliabue, E., Campiglio, M., and Pupa, S.M. (2000). Role of HER2 gene overexpression in breast carcinoma. J Cell Physiol *182*, 150-162.

Meyer, T., Xu, L., Chang, J., Liu, E.T., Craven, R.J., and Cance, W.G. (2003). Breast cancer cell line proliferation blocked by the Src-related Rak tyrosine kinase. Int J Cancer *104*, 139-146.

Miah, S., Martin, A., and Lukong, K.E. (2012). Constitutive activation of breast tumor kinase accelerates cell migration and tumor growth in vivo. Oncogenesis *1*, e11.

Mor, A., and Philips, M.R. (2006). Compartmentalized Ras/MAPK signaling. Annu Rev Immunol *24*, 771-800.

Oberg-Welsh, C., Anneren, C., and Welsh, M. (1998). Mutation of C-terminal tyrosine residues Y497/Y504 of the Src-family member Bsk/Iyk decreases NIH3T3 cell proliferation. Growth Factors *16*, 111-124.

Ogunbolude, Y., Dai, C., Bagu, E.T., Goel, R.K., Miah, S., MacAusland-Berg, J., Ng, C.Y., Chibbar, R., Napper, S., Raptis, L., *et al.* (2017a). FRK inhibits breast cancer cell migration and invasion by suppressing epithelial-mesenchymal transition. Oncotarget *8*, 113034-113065.

Paul, M.K., and Mukhopadhyay, A.K. (2004). Tyrosine kinase - Role and significance in Cancer. Int J Med Sci *1*, 101-115.

Pearson, G., Robinson, F., Beers Gibson, T., Xu, B.E., Karandikar, M., Berman, K., and Cobb, M.H. (2001). Mitogen-activated protein (MAP) kinase pathways: regulation and physiological functions. Endocr Rev *22*, 153-183.

Pilati, C., Letouze, E., Nault, J.C., Imbeaud, S., Boulai, A., Calderaro, J., Poussin, K., Franconi, A., Couchy, G., Morcrette, G., *et al.* (2014). Genomic profiling of hepatocellular adenomas reveals recurrent FRK-activating mutations and the mechanisms of malignant transformation. Cancer Cell *25*, 428-441.

Pimienta, G., and Pascual, J. (2007). Canonical and alternative MAPK signaling. Cell Cycle *6*, 2628-2632.

Qiu, H., and Miller, W.T. (2002). Regulation of the nonreceptor tyrosine kinase Brk by autophosphorylation and by autoinhibition. J Biol Chem *277*, 34634-34641.

Rawlings, J.S., Rosler, K.M., and Harrison, D.A. (2004). The JAK/STAT signaling pathway. J Cell Sci *117*, 1281-1283.

Ren, R., Mayer, B.J., Cicchetti, P., and Baltimore, D. (1993). Identification of a ten-amino acid proline-rich SH3 binding site. Science *259*, 1157-1161.

Robinson, D.R., Wu, Y.M., and Lin, S.F. (2000). The protein tyrosine kinase family of the human genome. Oncogene *19*, 5548-5557.

Rous, P. (1911). A Sarcoma of the Fowl Transmissible by an Agent Separable from the Tumor Cells. J Exp Med *13*, 397-411.

Russell, R.B., Breed, J., and Barton, G.J. (1992). Conservation analysis and structure prediction of the SH2 family of phosphotyrosine binding domains. FEBS Lett *304*, 15-20.

Sadowski, I., Stone, J.C., and Pawson, T. (1986). A noncatalytic domain conserved among cytoplasmic protein-tyrosine kinases modifies the kinase function and transforming activity of Fujinami sarcoma virus P130gag-fps. Mol Cell Biol *6*, 4396-4408.

Saksela, K., and Permi, P. (2012). SH3 domain ligand binding: What's the consensus and where's the specificity? FEBS Lett *586*, 2609-2614.

Serfas, M.S., and Tyner, A.L. (2003). Brk, Srm, Frk, and Src42A form a distinct family of intracellular Src-like tyrosine kinases. Oncol Res *13*, 409-419.

Shi, Q., Song, X., Wang, J., Gu, J., Zhang, W., Hu, J., Zhou, X., and Yu, R. (2015). FRK inhibits migration and invasion of human glioma cells by promoting N-cadherin/beta-catenin complex formation. J Mol Neurosci *55*, 32-41.

Smart, J.E., Oppermann, H., Czernilofsky, A.P., Purchio, A.F., Erikson, R.L., and Bishop, J.M. (1981). Characterization of sites for tyrosine phosphorylation in the transforming protein of Rous sarcoma virus (pp60v-src) and its normal cellular homologue (pp60c-src). Proc Natl Acad Sci U S A *78*, 6013-6017.

Snouwaert, J.N., Gowen, L.C., Latour, A.M., Mohn, A.R., Xiao, A., DiBiase, L., and Koller, B.H. (1999). BRCA1 deficient embryonic stem cells display a decreased homologous recombination frequency and an increased frequency of non-homologous recombination that is corrected by expression of a brca1 transgene. Oncogene *18*, 7900-7907.

Sorkin, A., and Goh, L.K. (2009). Endocytosis and intracellular trafficking of ErbBs. Experimental Cell Research *315*, 683-696.

Subramaniam, A., Shanmugam, M.K., Perumal, E., Li, F., Nachiyappan, A., Dai, X., Swamy, S.N., Ahn, K.S., Kumar, A.P., Tan, B.K., *et al.* (2013). Potential role of signal transducer and activator of transcription (STAT)3 signaling pathway in inflammation, survival, proliferation and invasion of hepatocellular carcinoma. Biochim Biophys Acta *1835*, 46-60.

Summy, J.M., and Gallick, G.E. (2003). Src family kinases in tumor progression and metastasis. Cancer Metastasis Rev *22*, 337-358.

Thangaraju, M., Kaufmann, S.H., and Couch, F.J. (2000). BRCA1 facilitates stress-induced apoptosis in breast and ovarian cancer cell lines. J Biol Chem *275*, 33487-33496.

Tsui, T., and Miller, W.T. (2015). Cancer-Associated Mutations in Breast Tumor Kinase/PTK6 Differentially Affect Enzyme Activity and Substrate Recognition. Biochemistry *54*, 3173-3182.

Waksman, G., Kominos, D., Robertson, S.C., Pant, N., Baltimore, D., Birge, R.B., Cowburn, D., Hanafusa, H., Mayer, B.J., Overduin, M., *et al.* (1992). Crystal structure of the phosphotyrosine recognition domain SH2 of v-src complexed with tyrosine-phosphorylated peptides. Nature *358*, 646-653.

Weinberg, R.A. (1995). The Retinoblastoma Protein and Cell-Cycle Control. Cell *81*, 323-330.

Welsh, M., Welsh, C., Ekman, M., Dixelius, J., Hagerkvist, R., Anneren, C., Akerblom, B., Mahboobi, S., Chandrasekharan, S., and Liu, E.T. (2004). The tyrosine kinase FRK/RAK participates in cytokine-induced islet cell cytotoxicity. Biochem J *382*, 261-268.

Wennerberg, K., Rossman, K.L., and Der, C.J. (2005). The Ras superfamily at a glance. J Cell Sci *118*, 843-846.

Weston, C.R., and Davis, R.J. (2002). The JNK signal transduction pathway. Curr Opin Genet Dev *12*, 14-21.

Xu, B., Kim, S., and Kastan, M.B. (2001). Involvement of Brca1 in S-phase and G(2)-phase checkpoints after ionizing irradiation. Mol Cell Biol *21*, 3445-3450.

Yim, E.K., Peng, G., Dai, H., Hu, R., Li, K., Lu, Y., Mills, G.B., Meric-Bernstam, F., Hennessy, B.T., Craven, R.J., *et al.* (2009). Rak functions as a tumor suppressor by regulating PTEN protein stability and function. Cancer Cell *15*, 304-314.

Yu, H., Chen, J.K., Feng, S., Dalgarno, D.C., Brauer, A.W., and Schreiber, S.L. (1994). Structural basis for the binding of proline-rich peptides to SH3 domains. Cell *76*, 933-945.

Yu, H., and Jove, R. (2004). The STATs of cancer--new molecular targets come of age. Nat Rev Cancer *4*, 97-105.

Zalutsky, M.R. (1997). Growth factor receptors as molecular targets for cancer diagnosis and therapy. Q J Nucl Med *41*, 71-77.

Zhao, B., Tan, P.H., Li, S.S., and Pei, D. (2013). Systematic characterization of the specificity of the SH2 domains of cytoplasmic tyrosine kinases. J Proteomics *81*, 56-69.

Zhou, X., Hua, L., Zhang, W., Zhu, M., Shi, Q., Li, F., Zhang, L., Song, C., and Yu, R. (2012). FRK controls migration and invasion of human glioma cells by regulating JNK/c-Jun signaling. J Neurooncol *110*, 9-19.